

# Covalently Bonded Fluorine as a $\sigma$ -Donor for Groups I and II Metal Ions in Partially Fluorinated Macrocycles<sup>‡</sup>

Herbert Plenio\* and Ralph Diodone

Contribution from the Institut für Anorganische und Analytische Chemie,  
Albertstrasse 21, 79104 Freiburg, Germany

Received August 24, 1995<sup>⊗</sup>

**Abstract:** Novel fluoro cryptands and fluoro crown ethers were synthesized in good yields in the reactions of 1,3-bis(bromomethyl)-2-fluorobenzene with diaza-18-crown-6 [the resulting two macrocycles are abbreviated as  $\text{FN}_2\text{O}_4$  (1 + 1 product) and  $(\text{FN}_2\text{O}_4)_2$  (2 + 2 product)], diaza-15-crown-5 [product abbreviated as  $\text{FN}_2\text{O}_3$ ], aza-(3*n*)-crown-(*n*) (*n* = 4, 5, 6) [ $\text{F}(\text{NO}_3)_2$ ,  $\text{F}(\text{NO}_4)_2$ ,  $\text{F}(\text{NO}_5)_2$ ], and the potassium salts of tetraethyleneglycol [ $\text{FO}_5$ ] or pentaethylene glycol [ $\text{FO}_6$ ] and in the reaction of 1-(bromomethyl)-3-methyl-2-fluorobenzene with aza-15-crown-5 [ $\text{FO}_4$ ]. The analogous reactions of 1,3-bis(bromomethyl)benzene with diaza-18-crown-6 [ $\text{HN}_2\text{O}_4$ ], diaza-15-crown-5 [ $\text{HN}_2\text{O}_3$ ], and the potassium salt of tetraethylene glycol [ $\text{HO}_5$ ] led to the isolation of closely related fluorine-free cryptands and crown ethers. The  $^{19}\text{F}$  NMR resonances of the fluoro macrocycles shift upon complexation of metal ions by between  $\Delta\delta = -18.2$  ppm and  $\Delta\delta = +8.5$  ppm relative to those of the respective free ligands. To explain the unexpected high-field shifts  $\Delta\delta$  of most metal complexes, a qualitative model is proposed which considers conformational rearrangements of the oxyethylene chain to be mainly responsible for the  $\Delta\delta$  values, with the deshielding effect of the positive charge of the metal ions being smaller in most cases. It was demonstrated that the  $^1J_{\text{CF}}$  coupling constants can be used to gauge the strength of metal–fluorine interactions since the values for  $^1J_{\text{CF}}$  range from 253 Hz ( $\text{FN}_2\text{O}_4$ ) to 238.5 Hz ( $\text{Li}^+\cdot\text{FN}_2\text{O}_4$ ), 242 Hz ( $\text{Na}^+\cdot\text{FN}_2\text{O}_4$ ), 246.5 Hz ( $\text{K}^+\cdot\text{FN}_2\text{O}_4$ ), and 249 Hz ( $\text{Rb}^+\cdot\text{FN}_2\text{O}_4$ ). The larger the metal ion the less it is able to migrate into the cavity and contact the C–F unit. The stability constants of the metal complexes of the fluoro macrocycles and their fluorine free relatives were determined by picrate extraction experiments and NMR competition experiments. It is evident from both investigations that the fluorine-containing macrocycles form more stable metal complexes than the analogous fluorine free systems. This is taken as a proof for C–F to metal ion  $\sigma$ -donor bonds. It is significant that this stabilizing effect is only observed when the radii of the metal ion and macrocyclic cavity are complementary, since only then can the metal ion contact the C–F unit. The crystal structures of  $\text{FN}_2\text{O}_3$  and the metal complexes  $\text{Li}^+\cdot\text{FN}_2\text{O}_3$ ,  $\text{Li}^+\cdot\text{HN}_2\text{O}_3$ ,  $\text{Na}^+\cdot\text{FN}_2\text{O}_3$ ,  $\text{Na}^+\cdot\text{FO}_5$ , and  $\text{Na}^+\cdot\text{FNO}_4$  were determined. In the solid state structures of all metal complexes with the exception of  $\text{Na}^+\cdot\text{FNO}_4$ , short metal–fluorine distances are observed, which are approximately as long as the respective metal–oxygen distances and much shorter than the metal–N distances [ $\text{Li}^+\cdot\text{FN}_2\text{O}_3$ :  $\text{Li}^+\text{–F}$ , 203.5(5) pm;  $\text{Li}^+\text{–O}$ , 193.6(5), 201.3(5), 202.1(5) pm;  $\text{Li}^+\text{–N}$ , 239.4(5), 255.5(5) pm], [ $\text{Na}^+\cdot\text{FO}_5$ :  $\text{Na}^+\text{–F}$ , 237.4(5) pm], [ $\text{Na}^+\cdot\text{FN}_2\text{O}_3$ :  $\text{Na}^+\text{–F}$ , 257.5(2) pm]. A comparison of the structures of  $\text{Li}^+\cdot\text{FN}_2\text{O}_3$  and  $\text{Li}^+\cdot\text{HN}_2\text{O}_3$  illustrates the importance of fluorine coordination since this interaction is required to position the metal ion within the center of the cavity, whereas in  $\text{Li}^+\cdot\text{HN}_2\text{O}_3$  the cation is located on the outer edge of the cavity, completing its coordination sphere with one additional molecule of water.

## 1. Introduction

The Lewis basicity of covalently bonded oxygen, nitrogen, sulfur, and phosphorus in ethers, amines, thioethers, and phosphanes is essential for the ability of such donor atoms to bind electron-deficient metal ions and constitutes the basis of coordination chemistry.<sup>1</sup> However, weak acceptors such as the alkaline metal ions require very efficient donor units to compete successfully with polar solvent molecules. Only ligands which take advantage of the chelating effect or even better the macrocyclic effect in combination with the appropriate set of hard donor ligands are able to form stable complexes with group I metal ions.<sup>2</sup> Nature itself has been using this concept for ages in ionophores such as valinomycin,<sup>3</sup> and it was comparatively recent that work by Pedersen, Lehn, and Cram led to the

synthesis of related macrocyclic ligands (crown ethers, cryptands, and spherands) which form extremely stable complexes with alkaline metal ions.<sup>4</sup>

The ideal hard donor atom for these metal ions is oxygen, with nitrogen being much less effective. The high electronegativity, the small size, and hence the hardness<sup>5</sup> of fluorine<sup>6</sup> raise the idea of covalently bonded fluorine as a promising donor atom for alkaline metal ions. Scattered reports of such interactions in the solid state have appeared in the literature.<sup>7,8</sup> A systematic crystallographic data analysis of intermolecular fluorine–metal ion distances was undertaken by Glusker et al. in the early 1980s, whereupon it became clear that short fluorine–metal contacts are not unusual in the solid state. This

(4) (a) Pedersen, C. J. *J. Am. Chem. Soc.* **1967**, *89*, 7017. (b) Dietrich, B.; Viout, P.; Lehn, J.-M. *Macrocyclic Chemistry*; VCH: Weinheim, 1993. (c) Gokel, G. W. *Crown Ethers & Cryptands*; Royal Society of Chemistry: London, 1991. (d) Vögtle, F. *Supramolekulare Chemie*; Teubner Verlag: Stuttgart, 1993. (e) Cram, D. J. *Angew. Chem.*, **1988**, *100*, 1041; *Angew. Chem., Int. Ed. Engl.* **1988**, *27*, 1009.

(5) Sen, K. D., ed. *Chemical Hardness. Structure and Bonding*; Springer-Verlag: Berlin, New York, 1993; Vol. 80.

(6) (a) Bergstrom, D. E.; Swarling, D. J. *Fluorine-Containing Molecules: Structure, Reactivity, Synthesis and Applications*; VCH: Weinheim, 1988. (b) Liebman, J. F.; Greenberg, A.; Dolbier, W. R. *Fluorine-Containing Molecules*; VCH: Weinheim, 1988.

<sup>‡</sup> Dedicated to Prof. Dr. Dr. h.c. mult. H. W. Roesky on his 60th birthday.

<sup>⊗</sup> Abstract published in *Advance ACS Abstracts*, December 15, 1995.

(1) Wilkinson, G.; Gillard, R. D.; McCleverty, J. A., Eds. *Comprehensive Coordination Chemistry*; Pergamon Press: London 1987.

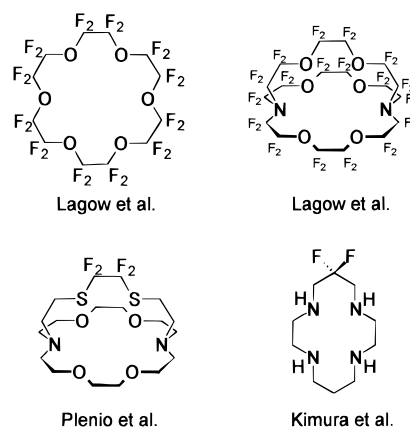
(2) Martell, A. E.; Hancock, R. D.; Motekaitis, R. J. *Coord. Chem. Rev.* **1994**, *133*, 39.

(3) (a) Marrone, T. J.; Merz, K. M. *J. Am. Chem. Soc.* **1995**, *117*, 779. (b) Gokel, G. W.; Nakano, A. In *Crown Compounds*; Cooper, S. R., Ed.; VCH: Weinheim, 1992; Chapter 1.

led Glusker to conclude that the C–F bond is capable of significant, if not prominent, interactions with both alkaline metal cations and proton donors.<sup>9,10</sup> Such interactions have also been made responsible for the large amount of unwanted metal fluorides formed in the pyrolysis of sodium fluoroalkoxides<sup>11</sup> and in the decomposition of cationic zirconocenes with the  $(C_6F_5)_3B(CH_3)^-$  counteranion.<sup>12</sup> However, it is important to realize that in all previous investigations close C–F–metal contacts were rather a byproduct of the packing of molecules and ions in the solid state and that no attempt has been made to rationally design ligands in which the donor ability of covalently bonded fluorine was exploited to coordinate metal ions.

The first perfluoro crown ethers were synthesized by Lagow et al. in the direct reaction of elemental fluorine with macrocyclic polyethers.<sup>13</sup> However, these compounds in common with those prepared by Farnham and Dixon et al.<sup>14</sup> are not capable of forming any complexes with metal ions, since the electron-withdrawing effect of the  $CF_2$  groups neutralizes the Lewis basicity of the ether units.<sup>15</sup> Kimura et al. have demonstrated that in macrocycles of the cyclam type a low content of fluorine is not harmful to the coordinating ability of

Chart 1. Fluorine-Containing Macrocycles



the nitrogen units.<sup>16</sup> We have recently shown that the synthesis of partially fluorinated crown ethers and cryptands from small fluorine-containing building blocks renders possible the formation of stable complexes with group I metals<sup>17</sup> (Chart 1). This approach, however, does not necessarily lead to close metal–fluorine interactions, and it was concluded that a better preorganization of the C–F unit was required to achieve this. We therefore set out to synthesize a chelating ligand related to EDTA in which a C–F bond is directed toward the potential site of metal coordination.<sup>18</sup> This approach has resulted in complexes in which alkaline earth metal ions closely interact with covalently bonded fluorine, resulting in shifts of the <sup>19</sup>F NMR resonances (relative to those metal free ligands) of up to 5 ppm. Such shifts can be observed easily due to the favorable NMR properties of the <sup>19</sup>F nucleus<sup>19</sup> and hold a potential for the development of a <sup>19</sup>F NMR metal ion sensor.<sup>20,21</sup> It could be demonstrated even more significantly that the presence of these interactions leads to small but significant increases in the stability of the metal complexes in solution relative to that of the analogous fluorine free complexes. Our main motivation for the study described here was to demonstrate that the C–F group can be an efficient donor unit in a sufficiently pre-organized array of donor atoms and that this effect is very significant for the strength of metal ion coordination in solution.

We report here the synthesis of novel fluoro cryptands, the analogous fluorine free ligands, and their metal complexes and a detailed investigation of the importance of C–F coordination in solution as well as in the solid state.<sup>22</sup>

## 2. Results and Discussion

### 2.1. Synthesis of Fluoro Crown Ethers and Fluoro Cryptands.

The basic building block for all fluoro macrocycles described in this work is 1,3-bis(bromomethyl)-2-fluorobenzene

(7)  $CF-Na^+$ : (a) Hurley, T. J.; Carrell, H. L.; Gupta, R. K.; Schwartz, J.; Glusker, J. P. *Arch. Biochem. Biophys.* **1979**, *193*, 478. (b) Carrell, H. L.; Glusker, J. P.; Villafranca, J. J.; Mildvan, A. S.; Dummel, R. J.; Kun, E. *Science* **1970**, *170*, 1412. (c) Vedavathi, B. M.; Vijayan, K. *Acta Crystallogr.* **1977**, *B33*, 946.  $CF-K^+$ : (d) Griffin, R. G.; Yeung, H.-N.; Laprade, M. D.; Waugh, J. S. *J. Chem. Phys.* **1973**, *59*, 777. (e) Mattes, R.; Gohler, D. J. *J. Mol. Struct.* **1980**, *68*, 59. (f) Spek, A. L.; Lenstra, A. T. H. *Cryst. Struct. Commun.* **1981**, *10*, 1527. (g) Purdy, A. P.; George, C. F.; Callahan, J. H. *Inorg. Chem.* **1991**, *30*, 2812. (h) Dias, H. V. R.; Lu, H. L.; Ratcliff, R. E.; Bott, S. G. *Inorg. Chem.* **1995**, *34*, 1975.  $CF-Rb^+$ : (i) McIntyre, W. M.; Zirakzadeh, M. *Acta Crystallogr.* **1964**, *17*, 1305. (j) Carrell, H. L.; Glusker, J. P. *Acta Crystallogr.* **1973**, *B29*, 674. (k) Fenton, D. E.; Nave, C.; Truter, M. R. *J. Chem. Soc., Dalton Trans.* **1973**, *21*, 2188.  $CF-Cs^+$ : (l) Bennet, M. J.; Cotton, F. A.; Legzdins, P.; Lippard, S. J. *Inorg. Chem.* **1968**, *7*, 1770.  $CF-Ca^{2+}$ : (m) Bradley, D. C.; Hasen, M.; Hursthouse, M. B.; Motevalli, M.; Khan, O. F. Z.; Pritchard, R. G.; Williams, J. O. *J. Chem. Soc., Chem. Commun.* **1992**, 575.  $CF-Ba^{2+}$ : (n) Purdy, A. P.; George, C. F. *Inorg. Chem.* **1991**, *30*, 1970. (o) Vincent, H.; Labrize, F.; Hubert-Pfalzgraf, L. G. *Polyhedron* **1994**, *13*, 3323.

(8) Examples of C–F to main group element, transition metal, and f-block element contacts in the solid state: (a) Yang, X.; Stern, C. L.; Marks, T. J. *Organometallics* **1991**, *10*, 840. (b) Brooker, S.; Bertel, N.; Stalke, D.; Noltemeyer, M.; Roesky, H. W.; Sheldrick, G. M.; Edelman, F. T. *Organometallics* **1992**, *11*, 192. (c) Edelman, F. T. *Comments Inorg. Chem.* **1992**, *12*, 259. (d) Uson, R.; Fornies, J.; Tomas, M. J. *J. Organomet. Chem.* **1988**, *358*, 525. (e) Simonov, Y. A.; Ivanov, V. I.; Ablov, A. V.; Malinovskii, T. I.; Milkova, L. N. *Koord. Khim.* **1975**, *1*, 716. (f) Simonov, Y. A.; Dvorkin, A. A.; Yablokov, Y. V.; Milkova, L. N.; Ablov, A. V. *Zh. Strukt. Khim.* **1978**, *19*, 175. (g) Catalia, R. M.; Cruz-Garriz, D.; Hills, A.; Hughes, D. L.; Richards, R. L.; Sosa, P.; Torrens, H. J. *J. Chem. Soc., Chem. Commun.* **1987**, 261. (h) Bradley, D. C.; Chudzynska, H.; Hammond, M. E.; Hursthouse, M. B.; Motevalli, M.; Ruowen, W. *Polyhedron* **1992**, *11*, 375. (i) Campbell, C.; Bott, S. G.; Larsen, R.; VanderSluys, W. G. *Inorg. Chem.* **1994**, *33*, 4950. (j) Schluter, R. D.; Cowley, A. H.; Atwood, D. A.; Jones, R. A.; Bond, M. R.; Carrano, C. J. *J. Am. Chem. Soc.* **1993**, *115*, 2070. (k) Horton, A. D.; Orpen, A. G. *Organometallics* **1991**, *10*, 3910.

(9) Murray-Rust, P.; Stalling, W. C.; Monti, C. T.; Preston, R. K.; Glusker, J. P. *J. Am. Chem. Soc.* **1983**, *105*, 3206.

(10) Kulawiec, R. J.; Crabtree, R. H. *Coord. Chem. Rev.* **1990**, *99*, 89.

(11) Samuels, J. A.; Lobkovsky, E. B.; Streib, W. E.; Foltling, K.; Huffman, J. C.; Zwanziger, J. W.; Caulton, K. G. *J. Am. Chem. Soc.* **1993**, *115*, 5093.

(12) Yang, X.; Stern, C. L.; Marks, T. J. *J. Am. Chem. Soc.* **1994**, *116*, 10015.

(13) (a) Lin, T. Y.; Bailey, W. I.; Lagow, R. J. *J. Chem. Soc., Chem. Commun.* **1985**, 1350. (b) Lin, T. Y.; Bailey, W. I.; Lagow, R. J. *Pure Appl. Chem.* **1988**, *60*, 473. (c) Clark, W. D.; Lin, T. Y.; Maleknia, S. D.; Lagow, R. J. *J. Org. Chem.* **1990**, *55*, 5933. (d) Lin, T. Y.; Lagow, R. J. *J. Chem. Soc., Chem. Commun.* **1991**, 12.

(14) (a) Farnham, W. B.; Roe, D. C.; Dixon, D. D.; Calabrese, J. C.; Harlow, R. L. *J. Am. Chem. Soc.* **1990**, *112*, 7707. (b) Hung, M. H.; Farnham, W. B.; Feiring, A. E.; Rozen, S. J. *J. Am. Chem. Soc.* **1993**, *115*, 8954.

(15) Lin, T. Y.; Lin, W. H.; Clark, W. D.; Lagow, R. J.; Larson, S. B.; Simonsen, S. H.; Lynch, V. M.; Brodbelt, J. S.; Maleknia, S. D.; Liou, C. C. *J. Am. Chem. Soc.* **1994**, *116*, 5172.

(16) Shionoya, M.; Kimura, E.; Iitaka, Y. *J. Am. Chem. Soc.* **1990**, *112*, 9237.

(17) Plenio, H. *Inorg. Chem.* **1994**, *33*, 6123.

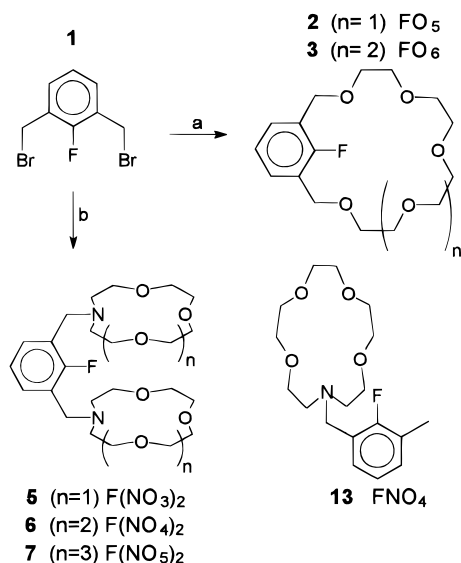
(18) Plenio, H.; Burth, D. *J. Chem. Soc., Chem. Commun.* **1994**, 2297.

(19) *Multinuclear NMR Spectroscopy*; Mason, J., Ed.; Plenum Press: New York, 1987.

(20) (a) Prior, M. J. W.; Maxwell, R. J.; Griffiths, J. R. In *In Vivo Magnetic Resonance Spectroscopy III. NMR Basic Principles and Progress*; Springer Verlag: Berlin, 1992; Vol. 28, pp 102–130. (b) Ochsner-Bruderer, M.; Fleck, T. *Nachr. Chem., Tech. Lab.* **1993**, *41*, 997.

(21) (a) Smith, G. A.; Kirschenlohr, H. L.; Metcalfe, J. C.; Clarke, S. D. *J. Chem. Soc., Perkin Trans. 2* **1993**, 1205. (b) Smith, G. A.; Hesketh, R. T.; Metcalfe, J. C.; Feeney, J.; Morris, P. G. *Proc. Natl. Acad. Sci. U.S.A.* **1983**, *80*, 7178. (c) Smith, G. A.; Morris, P. G.; Hesketh, T. R.; Metcalfe, J. C. *Biochim. Biophys. Acta* **1986**, *889*, 72.

(22) A preliminary account of this work has been published: Plenio, H.; Diodone, R. *Angew. Chem.* **1994**, *106*, 2267; *Angew. Chem., Int. Ed. Engl.* **1994**, *33*, 2175.

**Scheme 1.** Synthesis of the Fluoro Crown Ethers<sup>a</sup>

<sup>a</sup> (a)  $\text{KO}(\text{C}_2\text{H}_4\text{O})_x\text{C}_2\text{H}_4\text{OK}$  ( $x=3, 4$ ); (b)  $\text{N}-(3n+9)\text{-C}-(n+3)$  ( $n=1, 2, 3$ ),  $\text{Na}_2\text{CO}_3$ ,  $\text{CH}_3\text{CN}$ . **13** was prepared from the fluoroxylene monobromide and  $\text{N-15-C-5}$ .

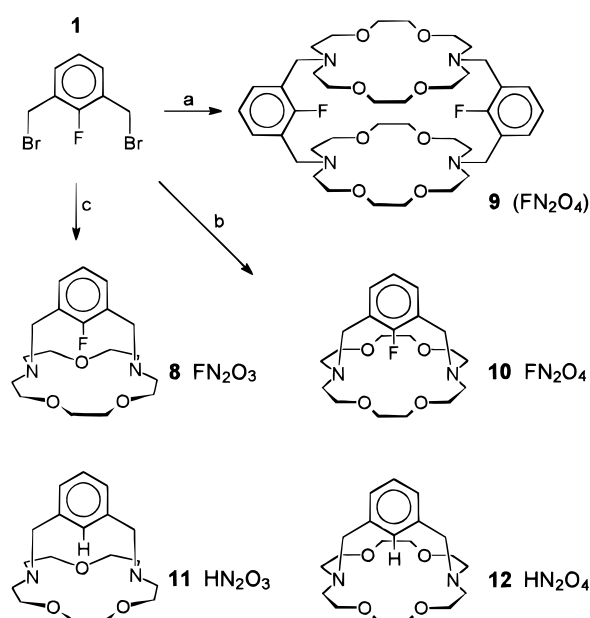
(**1**),<sup>23</sup> whose rigid six-membered ring renders it possible to orient the C–F bond such that it is pointing toward the center of the macrocycle, the potential site of the metal ion. The simple crown ethers  $\text{FO}_5$  and  $\text{FO}_6$ <sup>24</sup> can be prepared in the reaction of **1** with the potassium alcoholates of tetraethylene glycol or pentaethylene glycol in yields of 57% and 45%, respectively (Scheme 1). This condensation is carried out in the same manner as described by Reinhoudt et al. for the synthesis of crown ether  $\text{HO}_5$  derived from 1,3-bis(bromomethyl)benzene.<sup>25</sup> The reactions of the dibromide **1** with aza-( $3n+9$ )-crown-( $n+3$ ) ( $n=1, 2, 3$ ) in the presence of  $\text{Na}_2\text{CO}_3$  result in the formation of the bis-crown ethers  $\text{F}(\text{NO}_3)_2$ ,  $\text{F}(\text{NO}_4)_2$ , and  $\text{F}(\text{NO}_5)_2$  in yields between 75% and 88%. The aza-15-crown-5 derivative  $\text{FNO}_4$  was synthesized in the reaction of the mono(bromomethyl) derivative of **1** to determine whether significant metal–fluorine interactions are also possible in a lariat-type fluoro crown ether.

For the synthesis of the fluoro cryptands  $\text{FN}_2\text{O}_3$ ,  $\text{FN}_2\text{O}_4$ , and  $(\text{FN}_2\text{O}_4)_2$  it was not necessary to use high-dilution conditions (Scheme 2). Heating an equimolar mixture of diaza-15-crown-5 and **1** in acetonitrile under reflux in the presence of  $\text{Na}_2\text{CO}_3$  generates the desired 1 + 1 addition product  $\text{FN}_2\text{O}_3$  in 51% yield. On the other hand, the reaction of diaza-18-crown-6 with **1** under exactly the same conditions results mainly in the formation of the 2 + 2 condensation product  $(\text{FN}_2\text{O}_4)_2$ , with only minor amounts of the desired 1 + 1 product formed. However, using the larger templating ion  $\text{K}^+$  instead of  $\text{Na}^+$  unexpectedly leads to the formation of the smaller macrocycle  $\text{FN}_2\text{O}_4$ . The major product of the reaction of diaza-18-crown-6 with **1** in the presence of  $\text{KBr}/\text{K}_2\text{CO}_3$  is the 1 + 1 product (34% yield)  $\text{FN}_2\text{O}_4$  together with smaller amounts of the 2 + 2 product (21% yield, maximum yield 50%!)  $(\text{FN}_2\text{O}_4)_2$ . The analogous fluorine free cryptands  $\text{HN}_2\text{O}_3$  and  $\text{HN}_2\text{O}_4$  were prepared in a similar fashion.<sup>26</sup>

(23) Nasir, M. S.; Cohen, B. J.; Karlin, K. D. *J. Am. Chem. Soc.* **1992**, *114*, 2482.

(24) The short forms used in this paper to denote the fluoro macrocycles are derived from the number and the atom types of donor atoms within the respective ring system. Thus,  $\text{FO}_5$  stands for 21-fluoro-3,6,9,12,15-pentaoxabicyclo[15.3.11.17]heneicosa-1(21),17,19-triene, and  $\text{HO}_5$  which contains hydrogen instead of fluorine is an otherwise analogous macrocycle.

(25) Gray, R. T.; Reinhoudt, D. N.; Smit, C. J.; Veenstra, Ms. I. *Recueil* **1976**, *95*, 258.

**Scheme 2.** Synthesis of the Fluoro Cryptands<sup>a</sup>

<sup>a</sup> (a)  $\text{N}_2\text{-18-C-6}$ ,  $\text{Na}_2\text{CO}_3$ ,  $\text{CH}_3\text{CN}$ ; (b)  $\text{N}_2\text{-18-C-6}$ ,  $\text{K}_2\text{CO}_3$ ,  $\text{CH}_3\text{CN}$ ; (c)  $\text{N}_2\text{-15-C-5}$ ,  $\text{Na}_2\text{CO}_3$ ,  $\text{CH}_3\text{CN}$ .

## 2.2. NMR Investigations. 2.2.1. <sup>19</sup>F NMR Spectroscopy.

The <sup>19</sup>F nucleus displays several useful properties such as high sensitivity (85% of <sup>1</sup>H), large signal dispersion, and the absence of a natural background and is thus an extremely useful tool for monitoring the complexation reactions of fluoro macrocycles.

The ready formation of complexes of groups I and II metal ions with the ligands described here is evidenced by substantial shifts  $\Delta\delta$  of the <sup>19</sup>F NMR resonances with respect to the free ligand, which amount to  $\Delta\delta = -18.2$  ppm for  $\text{Li}^+\cdot\text{FN}_2\text{O}_3$  and  $\Delta\delta = -11.9$  ppm for  $\text{Ca}^{2+}\cdot\text{FN}_2\text{O}_4$  (Table 1). To prove that these shifts originate exclusively from the formation of cation–crown ether complexes and not from an interaction of the cation with the  $\text{CFCl}_3$  reference or a change of solvent polarity, a control experiment was carried out. A  $\text{CD}_3\text{CN}$  solution of **1** together with a small amount of  $\text{CFCl}_3$  reference was titrated with 2 equiv of  $\text{NaClO}_4$  and the <sup>19</sup>F NMR shift of the fluoroxylene **1** relative to  $\text{CFCl}_3$  monitored. The difference between these two peaks as well as the absolute shifts (within the drift stability of the field) remains constant to within less than 0.1 ppm. It can thus be concluded that the  $\text{CFCl}_3$  reference is not spoiled by the presence of metal salts, and therefore all following <sup>19</sup>F NMR experiments were carried out in acetonitrile solvent using  $\text{CFCl}_3$  as a standard.

The complexation/decomplexation reactions of all crown ether complexes are fast on the NMR time scale, leading to a continuous shift of the NMR resonances upon addition of metal ions, but are in the slow exchange region for the cryptand metal ion complexes. Upon formation of metal complexes of the fluoro cryptands the <sup>19</sup>F NMR resonances are shifted toward higher field in most cases (Table 1). This seems somewhat surprising at first glance since incorporation of a cation into the cavity of a ligand should result in a deshielding of the NMR signals—especially in the case of the doubly charged alkaline earth metal ions.<sup>27</sup> However, the results obtained here show that this idea is too simple.

(26) (a) Krakowiak, K. E.; Bradshaw, J. S.; Dalley, M. K.; Zhu, C.; Yi, G.; Curtis, J. C.; Izatt, R. M. *J. Org. Chem.* **1992**, *57*, 3166. (b) Pietraszkiewicz, M.; Gasiorowski, R.; Kozbial, J. *J. Inclusion Phenom.* **1989**, *7*, 309.

(27) Live, D.; Chan, S. J. *J. Am. Chem. Soc.* **1976**, *98*, 3769.

**Table 1.**  $^{19}\text{F}$  NMR Shifts of the Fluoro Crown Ethers and Their Metal Complexes (Solvent Acetonitrile, Reference  $\text{CFCl}_3$ )<sup>d</sup>

	$\text{FO}_5$	$\text{FO}_6$	$\text{F}(\text{NO}_3)_2$	$\text{F}(\text{NO}_4)_2$	$\text{F}(\text{NO}_5)_2$	$\text{FN}_2\text{O}_3$	$(\text{FN}_2\text{O}_4)_2$	$\text{FN}_2\text{O}_4$
ligand	-121.27	-123.37	-123.63	-123.70	-123.78	-109.10	-124.46	-114.38
$\text{Li}^+{}^a$	+0.1		+4.5	+2.3	+4.4	-18.2		-12.8
$\text{Na}^+{}^a$	-4.5		-3.1	+1.6	-0.7	-5.1		-11.0
$\text{K}^+{}^a$	-2.2	-1.0 <sup>b</sup>	-0.5	+1.5	-1.9		<sup>c</sup>	-4.5 <sup>b</sup>
$\text{Rb}^+{}^b$	-1.5	+0.1	+1.5	+4.0	<sup>c</sup>		+5.4	-1.7
$\text{Cs}^+{}^b$		+2.0	+5.0	+5.5	+2.6	<sup>c</sup>		-4.6
$\text{Ca}^{2+}{}^a$	+0.1	+4.1	+7.0	+8.2	+8.6	-9.2		-11.9
$\text{Sr}^{2+}{}^a$	+0.1	+2.0	+6.7	+7.6	+8.5	-3.1		-9.5
$\text{Ba}^{2+}{}^a$	+3.6	+4.9	+6.4	+7.4	+7.9		+6.5	-5.1

<sup>a</sup>  $\text{ClO}_4$  salts. <sup>b</sup>  $\text{SO}_3\text{CF}_3$  salts. <sup>c</sup> Several species. <sup>d</sup> Shifts  $\Delta\delta$  (ppm) of the metal complexes are given relative to those of the respective free ligands.

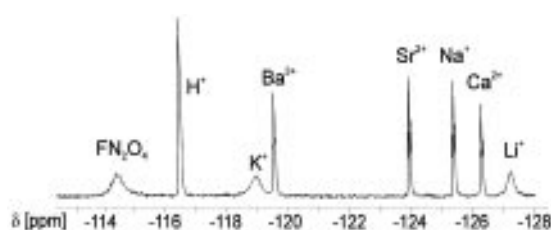


**Figure 1.**  $^{19}\text{F}$  NMR spectrum of a mixture of  $\text{FN}_2\text{O}_4$  and  $\text{Li}^+$ ,  $\text{Na}^+$ ,  $\text{K}^+$ ,  $\text{Rb}^+$ ,  $\text{Mg}^{2+}$ ,  $\text{Ca}^{2+}$ ,  $\text{Sr}^{2+}$ , and  $\text{Ba}^{2+}$  (all metal ions as their  $\text{CF}_3\text{SO}_3^-$  salts,  $\text{H}^+$  due to  $\text{Mg}^{2+}/\text{H}_2\text{O}$ ).

It is apparent from the data listed in Table 1 that the ligands described here can be divided into two groups on the basis of their  $^{19}\text{F}$  NMR shifts.  $\text{FO}_5$ ,  $\text{FO}_6$ ,  $\text{F}(\text{NO}_3)_2$ ,  $\text{F}(\text{NO}_4)_2$ ,  $\text{F}(\text{NO}_5)_2$ , and  $(\text{FN}_2\text{O}_4)_2$  belong to the first class which is characterized by  $\delta$ -values between  $-121.3$  and  $-124.5$  ppm and will be called conformationally relaxed macrocycles from now on. The other group, which will be termed conformationally strained ligands, is made up from  $\text{FN}_2\text{O}_3$  and  $\text{FN}_2\text{O}_4$  since their  $^{19}\text{F}$  NMR shifts at  $\delta = -109.10$  and  $-114.38$  ppm, respectively, are rather different from those of the first group and seem to be dominated by the shielding influence of the crown ether unit. This is in accord with the observation that molecular motion in a flexible chain leads to an appreciable reduction of the van der Waals shielding term.<sup>28</sup>

Upon comparing the  $^{19}\text{F}$  NMR spectra of the complexes of  $\text{FN}_2\text{O}_4$  with groups I and II metal ions, it is apparent that the ordering of the  $\Delta\delta$  values is according to the ionic radii<sup>29</sup> of the cations and not according to charge or a charge/density ratio, since within the pairs of complexes of  $\text{FN}_2\text{O}_4$  with  $\text{Na}^+/\text{Ca}^{2+}$  and  $\text{K}^+/\text{Ba}^{2+}$  the  $\Delta\delta$  values are quite similar (Figure 1<sup>30</sup>).

It is remarkable that, in all strained ligands, the formation of metal complexes leads to a high-field shift of the  $^{19}\text{F}$  NMR signals, whereas in the relaxed macrocycles this is only the case for the complexes of group I metal ions. In the 18-membered ring  $\text{FO}_5$  only the monocationic metal ions induce high-field shifts, whereas for  $\text{Ca}^{2+}$  and  $\text{Sr}^{2+}$  two counteracting effects seem to neutralize each other, resulting in an almost zero overall shift of the  $^{19}\text{F}$  NMR resonances. In  $\text{FO}_5\cdot\text{Ba}^{2+}$  on the other hand the deshielding influence of the doubly charged metal ion is dominating. The effect of the positive charge is even more pronounced in the 21-membered ring of  $\text{FO}_6$ , which gives low-field shifts for all doubly charged alkaline earth metal ions and also for some group I metal ions. The same holds true for the complexes of  $\text{F}(\text{NO}_3)_2$ ,  $\text{F}(\text{NO}_4)_2$ , and  $\text{F}(\text{NO}_5)_2$  which experience the expected deshielding effect with most metal ions.

To account for the observed shifts of the  $^{19}\text{F}$  NMR resonances upon coordination of metal ions, we present here a qualitative model in which charge is only one of several mechanisms responsible for the observed NMR shifts in macrocyclic metal complexes. It is known that the shifts of the  $^{13}\text{C}$  NMR resonances are very sensitive to conformational changes,<sup>31</sup> consequently upon addition of metal salts to, for example, ferrocene crown ethers this structural effect is more important for the  $\Delta\delta$  values than the positive charge of the metal ion.<sup>32,33</sup> While this explanation is acceptable for carbon, it could be argued that this can hardly hold true for a fluorine atom which is directly bonded to the positive ion.

We consider at least two factors to be responsible for the high-field shifts of the  $^{19}\text{F}$  NMR resonances of  $\text{FN}_2\text{O}_3$  and  $\text{FN}_2\text{O}_4$  upon addition of metal ions: a close interaction of the metal ion with the  $^{19}\text{F}$  nucleus and a conformational rearrangement as well as a stiffening of the polyether chain due to the migration of a metal ion into the cavity of the macrocycle. Obviously the latter effect seems to be the dominant mechanism responsible for the  $^{19}\text{F}$  NMR shifts in the strained cryptands  $\text{FN}_2\text{O}_3$  and  $\text{FN}_2\text{O}_4$ . However, when looking at the  $^{19}\text{F}$  NMR shifts of conformationally relaxed ligands, it becomes apparent that both processes must be of significance, since in several complexes of  $\text{FO}_5$ ,  $\text{FO}_6$ ,  $\text{F}(\text{NO}_3)_2$ ,  $\text{F}(\text{NO}_4)_2$ , and  $\text{F}(\text{NO}_5)_2$  shifts of the  $^{19}\text{F}$  NMR signals to lower field are observed. It seems as if the effect due to the conformational rearrangement is less important in the relaxed ligands and that the deshielding influence of the positively charged metal ions on the  $^{19}\text{F}$  NMR resonances slowly takes over.

The varying shielding contributions of the polyether chains in the conformationally relaxed or strained macrocycles and in the rigid chain of the metal complexes together with the counteracting deshielding influence of the positive charge of the metal cations can be seen in the context of the ongoing discussion, whether the shielding of  $^{19}\text{F}$  NMR resonances in proteins is dominated by electrostatic fields<sup>34</sup> or whether van der Waals shielding<sup>35</sup> also plays an important role.

It should also be mentioned that Reinhoudt et al. have presented an explanation to account for the unusual shifts of the  $^1\text{H}$  NMR resonances in the fluorine free crown ethers  $\text{HO}_5$  and  $\text{HO}_6$  which is based on a size-fit relation of cavity and cation radii and the formation of different anion-cation pairs.<sup>36</sup> Our discussion of the  $^{19}\text{F}$  NMR shifts so far has not taken into

(31) (a) Bright, D.; Truter, M. R. *J. Chem. Soc. B* **1970**, 1544. (b) Dale, J. *Isr. J. Chem.* **1980**, *20*, 3.

(32) Plenio, H.; El-Desoky, H.; Heinze, J. *Chem. Ber.* **1993**, *126*, 2403.

(33) Ingham, S. L.; Long, N. J. *Angew. Chem.* **1994**, *106*, 1847; *Angew. Chem., Int. Ed. Engl.* **1994**, *33*, 1752.

(34) (a) deDios, A. C.; Pearson, J. G.; Oldfield, E. *Science* **1993**, *260*, 1491. (b) Pearson, J. G.; Oldfield, E.; Lee, F. S.; Warshel, A. *J. Am. Chem. Soc.* **1993**, *115*, 6851. (c) deDios, A. C.; Oldfield, E. *J. Am. Chem. Soc.* **1994**, *116*, 7453.

(35) Chambers, S. E.; Lau, E. Y.; Gerig, J. T. *J. Am. Chem. Soc.* **1994**, *116*, 3603.

(28) Gregory, D. H.; Gerig, J. T. *Biopolymers* **1991**, *31*, 845.

(29) Shannon, R. D. *Acta. Crystallogr.* **1976**, *A22*, 751.

(30) The broadening of several  $^{19}\text{F}$  NMR resonances is only observed in the mixture of seven metal salts with  $\text{FN}_2\text{O}_4$ ; the individual metal complexes with this ligand display narrow NMR resonances at room temperature.

account the possibility of differing degrees of anion–cation contacts in cryptands and crown ethers which might well be of significance in a less polar solvent such as  $\text{CD}_3\text{CN}$ .<sup>37,38</sup> For the crown ether complexes anion–cation contacts appear more likely, whereas a metal ion bonded to the cryptand is probably well shielded from its environment. We have therefore determined the  $^{19}\text{F}$  NMR shifts of the respective complexes of  $\text{FO}_5$  and  $\text{FN}_2\text{O}_4$  with  $\text{NaClO}_4$  and  $\text{NaBPh}_4$  though only  $\text{BPh}_4^-$  can be considered a truly noncoordinating anion.<sup>39</sup> However, in both cases the shifts of the  $^{19}\text{F}$  NMR resonances of the complexes with  $\text{NaClO}_4$  and  $\text{NaBPh}_4$  are identical to within less than  $\pm 0.1$  ppm. It can thus be concluded that anion–cation interactions are not of significance for the  $^{19}\text{F}$  NMR shifts with such anions.

It is interesting to consider the effect of  $\text{Li}^+$  and  $\text{Na}^+$  addition on the  $^{19}\text{F}$  NMR resonances of  $\text{FNO}_4$  ( $-123.30$  ppm), since this ligand lacks the degree of preorganization found in the fluoro cryptands. Addition of  $\text{LiClO}_4$  results in a continuous shift of the resonances which comes to a halt when approximately equimolar amounts of ligand and salt are present ( $\Delta\delta = -1.4$  ppm); addition of  $\text{NaClO}_4$  ( $\Delta\delta = -0.4$  ppm) or  $\text{Ca}(\text{ClO}_4)_2$  ( $\Delta\delta = +4.1$  ppm) gives less negative shifts. These  $\Delta\delta$  values are in line with the model of a relaxed macrocycle in which the positive charge of the alkaline metal ions can almost compensate for the effects due to the rearrangement of the polyether chain. It should be mentioned that this interpretation only makes sense when a bonding interaction of the metal ions with fluorine is present in solution, which was not observed in the crystal structure of  $\text{HNO}_4 \cdot \text{NaClO}_4$  (see the X-ray Crystal Structures section). To prove this, we have performed NMR competition experiments in which equimolar amounts of  $\text{HNO}_4$  and  $\text{FNO}_4$  were titrated with  $\text{LiClO}_4$  or  $\text{NaClO}_4$ . It is evident from these experiments that there is a very small stabilization ( $+7\%$ ) of the fluorine-containing complex of  $\text{FNO}_4$  relative to that of  $\text{HNO}_4$  (see also the Stability Constants section and  $^{13}\text{C}$  NMR section).

According to the concept of strained and relaxed macrocycles and the dominance of conformational rearrangement for the  $\Delta\delta$  values observed in the  $^{19}\text{F}$  NMR spectra, close fluorine metal contacts (fluorine–metal  $\sigma$ -donor bonds) should only be of secondary importance for the  $^{19}\text{F}$  NMR shifts. The question then is how we recognize such contacts *in solution* by NMR, ignoring all evidence from crystal structure analysis.

One criterion for close metal–fluorine contacts would be the observation of a scalar coupling constant. Promising candidates are the complexes of  $^{133}\text{Cs}$ , which is highly abundant in spin  $1/2$  nuclei and  $^6,7\text{Li}$  with spins  $1$  and  $3/2$ , respectively. Indeed a magnetic coupling of the nuclear spins was observed in  $\text{FN}_2\text{O}_3 \cdot ^7\text{Li}^+$  ( $J_{\text{LiF}} = 19$  Hz,  $\Delta\delta = -18.2$  ppm), but neither in  $\text{FN}_2\text{O}_4 \cdot \text{Li}^+$  ( $\Delta\delta = -12.8$  ppm) nor in any complex of  $\text{Cs}^+$  (not even at low temperatures). To understand whether these are through-space couplings or direct couplings due to  $\sigma$ -donor bonds, it would be helpful to know the sign of the  $^1J$  coupling, but at this point one can only take guesses, since a positive sign was found in  $\text{LiF}$ ,<sup>40</sup> whereas it is recognized as an empirical rule that atoms with lone pairs display a negative  $^1J$  coupling constant.<sup>41</sup>

(36) Reinhoudt, D. N.; Gray, R. T.; DeJong, F.; Smit, C. J. *Tetrahedron* **1977**, *33*, 563.

(37) (a) Troxler, L.; Wipff, G. *J. Am. Chem. Soc.* **1994**, *116*, 1468. (b) Wipff, G. *J. Coord. Chem.* **1992**, *27*, 7.

(38) Kunz, W.; Calmette, P.; Turq, P.; Cartailier, T.; Morel-Desroisiers, N.; Morel, J. P. *J. Chem. Phys.* **1992**, *97*, 5467.

(39) Erlich, R. H.; Popov, A. I. *J. Am. Chem. Soc.* **1971**, *93*, 5620.

It is worth noting that spin–spin coupling of a neutral C–F unit to  $^6,7\text{Li}^+$  to the best of our knowledge has not been observed before,<sup>42</sup> but that one of C–F–Cs<sup>+</sup> was found in a close ion pair.<sup>43</sup> Examples of  $^6,7\text{Li}$ – $^{19}\text{F}$  coupling in  $\text{Si-F-Li-N}^{44}$  and  $\text{P-F-Li-N}^{45}$  four-membered rings are known, but these compounds are better viewed as preformed  $\text{LiF}$  trapped in the course of iminosilane or iminophosphane formation.

**2.2.2.  $^1\text{H}$  NMR.** The  $^1\text{H}$  NMR spectra of the free cryptands as well as those of the corresponding metal complexes are characterized by very complex multiplet patterns. The hydrogen atoms within all  $\text{CH}_2$  groups are unique (exo and endo with respect to the cavity); thus, each  $\text{OCH}_2\text{CH}_2\text{O}$  unit gives rise to high-order spectra of the ABCD type. The chemical shifts of the two hydrogen atoms of the benzylic  $\text{CH}_2$  groups, which are very close to the aromatic ring, typically differ by more than  $1$  ppm! The  $^1\text{H}$  NMR shifts of the hydrogen atoms within the oxyethylene ring will be influenced by different conformations and different positions of the chain with respect to the aromatic ring, and it is therefore difficult to single out any effect due to a metal ion. On the other hand the hydrogen nuclei in the 4-, 6-, and 5-positions of the aromatic rings should not suffer from such complicating effects, and it is not surprising that these  $^1\text{H}$  NMR resonances display the expected deshielding upon formation of metal complexes with the fluoro macrocycles.

The related crown ethers  $\text{HN}_2\text{O}_3$  and  $\text{HN}_2\text{O}_4$  were mainly synthesized to determine the stabilizing effect of fluorine coordination (see the Stability Constants section), but we were also intrigued whether formation of metal complexes with these ligands had a pronounced effect on the  $^1\text{H}$  NMR shifts. In the free ligand  $\text{HN}_2\text{O}_3$  the aromatic hydrogen atom pointing toward the center of the cavity is characterized by an unusual low-field signal at  $\delta = 8.86$  ppm. In the metal complexes of  $\text{HN}_2\text{O}_3$  a very pronounced high-field shift of this hydrogen resonance is observed ( $\text{Li}^+ \cdot \text{HN}_2\text{O}_3$  ( $\Delta\delta = -1.39$  ppm),  $\text{Na}^+ \cdot \text{HN}_2\text{O}_3$  ( $\Delta\delta = -1.23$  ppm), and  $\text{K}^+ \cdot \text{HN}_2\text{O}_3$  ( $\Delta\delta = -0.40$  ppm)). This shift depends on the size of the metal ion and reflects the trend found for the  $^{19}\text{F}$  NMR shifts in  $\text{FN}_2\text{O}_3$  and its metal complexes. This observation adds further weight to our interpretation that van der Waals shielding is dominant in the conformationally strained macrocycles.

**2.2.3.  $^{13}\text{C}$  NMR.** It would be very helpful if it was possible to detect the presence of close metal–fluorine interactions in solution by NMR spectroscopy. Attempts to correlate  $^{19}\text{F}$  or  $^{13}\text{C}$  NMR  $\Delta\delta$  values with the degree of cation–fluorine interaction in solution have only met with limited success. However, since the partial multiple bond character of the  $\text{sp}^2$  carbon bond with fluorine should be reduced upon coordination of fluorine to a metal ion, it was hoped for that changes in the  $^1J_{\text{CF}}$  coupling constant would be indicative of close metal–

(40) Lanolt-Börnstein. *Zahlenwerte und Funktionen aus Naturwiss. und Technik*; Springer Verlag: Berlin, 1974; Group II.

(41) Jameson, C. J. Spin-Spin Coupling. In *Multinuclear NMR*; Mason, J., Ed.; Plenum Press: New York, 1987.

(42) Berger, S.; Braun, S.; Kalinowski, H. O. *NMR-Spektroskopie von Nichtmetallen.  $^{19}\text{F}$ -NMR Spektroskopie*; Thieme Verlag: Stuttgart, 1994; Vol. 4.

(43) (a) Boyd, A. S. F.; Davidson, J. L.; McIntosh, C. H.; Leverd, P. C.; Lindsell, E.; Simpson, N. J. *J. Chem. Soc., Dalton Trans.* **1992**, 2531. (b) Davidson, J. L.; McIntosh, C. H.; Leverd, P. C.; Lindsell, W. E.; Simpson, N. J. *J. Chem. Soc., Dalton Trans.* **1994**, 2423.

(44) (a) Walter, S.; Klingebiel, U. *Coord. Chem. Rev.* **1994**, *130*, 481.

(b) Stalke, D.; Whitmire, K. H. *J. Chem. Soc., Chem. Commun.* **1990**, 833.

(c) Stalke, D.; Klingebiel, U.; Sheldrick, G. M. *Chem. Ber.* **1988**, *121*, 1457.

(45) Dries, M.; Winkler, U.; Imhof, W.; Zolnai, L.; Huttner, G. *Chem. Ber.* **1994**, *127*, 1031.

**Table 2.**  $^{13}\text{C}$  NMR Shifts (ppm) and  $^1J_{\text{CF}}$  (Coupling Constants, in Parentheses) (Hz) for the C–F Group of the Fluorinated Macrocycles and Their Respective Metal Complexes

	$\text{FN}_2\text{O}_3$	$\text{FN}_2\text{O}_4$	$\text{FO}_5$
ligand	164.39 (256)	161.64 (252)	161.64 (250.5)
$\text{Li}^+$	162.37 (238.5)	161.55 (238.5)	161.82 (250.5)
$\text{Na}^+$	162.35 (246.5)	161.00 (242.5)	161.98 (245)
$\text{K}^+$	163.34 (257)	161.41 (246.5)	160.99 (238)
$\text{Rb}^+$		161.90 (250)	161.14 (248)
$\text{Ca}^{2+}$	161.49 (239)	158.87 (230)	161.76 (241)
$\text{Sr}^{2+}$		159.46 (235.5)	160.17 (236)
$\text{Ba}^{2+}$		159.87 (238.5)	159.59 (240)

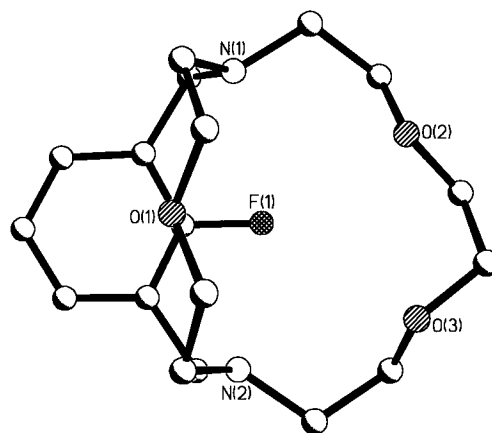
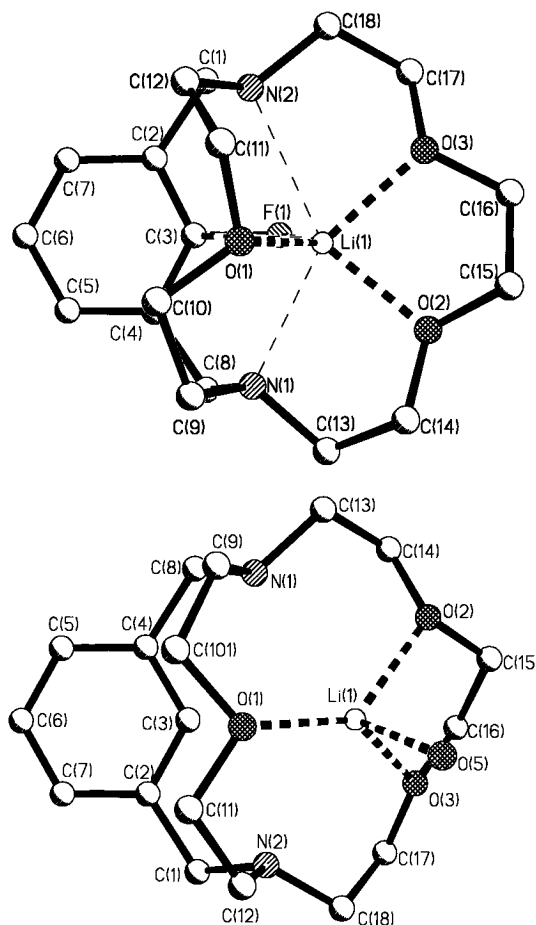
fluorine contacts in solution.<sup>46</sup> In Table 2 the values of the  $^1J_{\text{CF}}$  coupling constant and the  $^{13}\text{C}$  shift of this carbon in  $\text{FN}_2\text{O}_3$ ,  $\text{FN}_2\text{O}_4$ ,  $\text{FO}_5$ , and their respective metal complexes are listed. It can be seen that the  $^1J_{\text{CF}}$  coupling constants in the metal complexes are significantly smaller than in the free ligands. The smallest value of  $^1J_{\text{CF}} = 230$  Hz is observed in  $\text{Ca}^{2+}\cdot\text{FN}_2\text{O}_4$  and corresponds to a reduction in the coupling constant of 22 Hz. This effect is more pronounced the better the metal ion fits into the cavity and thus is able to contact fluorine. It is for this reason that an increase in the size of the metal ions leads to coupling constants which are close to those of the free ligand. Accordingly in  $\text{K}^+\cdot\text{FN}_2\text{O}_3$  and  $\text{Rb}^+\cdot\text{FN}_2\text{O}_4$  negligible metal–fluorine contacts exist as these ions obviously are too big to come in contact with fluorine which is located on the inside of the cavity.

It is interesting to compare the  $^1J_{\text{CF}}$  coupling constants for the different complexes of  $\text{FO}_5$  with the  $\Delta\delta$  values displayed in Table 2. Both  $\text{Li}^+\cdot\text{FO}_5$  and  $\text{Sr}^{2+}\cdot\text{FO}_5$  display  $\Delta\delta$  values close to zero—but for very different reasons! In the  $\text{Li}^+$  complex the fluorine–metal interactions are weak as evidenced by  $^1J_{\text{CF}} = 250.5$  Hz, whereas in the  $\text{Sr}^{2+}$  complex the  $\Delta\delta$  value close to zero is due to the fact that the shielding effect of the oxyethylene chain and the deshielding effect of the positive charge compensate to almost zero ( $^1J_{\text{CF}} = 236$  Hz). Judging from the coupling constants only, it seems as if the optimum metal–fluorine contact in  $\text{FO}_5$  complexes occurs in the case of  $\text{Sr}^{2+}$  and  $\text{K}^+$ , which is reasonable in terms of ring size. The decrease of  $^1J_{\text{CF}}$  in  $\text{FNO}_4\cdot\text{NaClO}_4$  ( $^1J_{\text{CF}} = 241$  Hz) relative to  $\text{FNO}_4$  ( $^1J_{\text{CF}} = 249$  Hz) is indicative of fluorine–metal interaction in this lariat type ligand.

**2.2.4.  $^{19}\text{F}$  CP-MAS NMR.** To build a bridge between X-ray crystal structures and solution NMR techniques and to learn whether the solid state structures of the macrocyclic metal complexes are good models for the behavior in solution, we have recorded solid state  $^{19}\text{F}$  MAS NMR spectra<sup>47</sup> of  $\text{FN}_2\text{O}_3$ ,  $\text{Li}^+\cdot\text{FN}_2\text{O}_3$ , and  $\text{Na}^+\cdot\text{FN}_2\text{O}_3$  (both complexes as  $\text{CF}_3\text{SO}_3$  salts).

The free ligand displays a resonance at  $-114$  ppm (referenced vs PTFE,  $-123.2$  ppm). In  $\text{Li}^+\cdot\text{FN}_2\text{O}_3$  the  $^{19}\text{F}$  signal is shifted to  $-132$  ppm, which corresponds to  $\Delta\delta = -18$  ppm. This  $\Delta\delta$  value is very close to the one observed for this complex in acetonitrile solution ( $\Delta\delta = -18.2$  ppm) and shows that the X-ray crystal structure is a good model for the species present in solution. For  $\text{Na}^+\cdot\text{FN}_2\text{O}_3$  the case is less clear cut since this metal ion does not induce any shift of the  $^{19}\text{F}$  MAS NMR signal; in both metal complexes the  $\text{CF}_3\text{SO}_3^-$  resonance is observed at  $-77.6$  ppm.

**2.3. X-Ray Crystal Structures.** **2.3.1. Structure of  $\text{FN}_2\text{O}_3$  (Figure 2).** The solid state structure of  $\text{FN}_2\text{O}_3$  was determined to assess the degree of structural preorganization upon comparison with the respective metal-containing complexes. The

**Figure 2.** X-ray crystal structure of  $\text{FN}_2\text{O}_3$  (hydrogen atoms omitted).**Figure 3.** X-ray crystal structures of  $\text{FN}_2\text{O}_3\cdot\text{Li}^+$  and  $\text{HN}_2\text{O}_3\cdot\text{Li}^+$  (hydrogen atoms omitted).

structural features of  $\text{FN}_2\text{O}_3$  are unremarkable except for the fact that the two methylene carbon atoms bonded to the planar six-membered ring are bent ca.  $8^\circ$  out of this plane toward the smaller oxyethylene chain. The fluorine atom in  $\text{FN}_2\text{O}_3$  is not buried between the two oxyethylene chains but sits on the outside next to the longer oxyethylene chain.

**2.3.2. Structures of  $\text{Li}^+\cdot\text{FN}_2\text{O}_3$  (Figure 3),  $\text{Li}^+\cdot\text{HN}_2\text{O}_3$  (Figure 3), and  $\text{Na}^+\cdot\text{FN}_2\text{O}_3$  (Figure 5).** To find out whether the presence of a C–F unit in the fluoro cryptands has any influence on the coordination geometry of lithium, we have determined the X-ray crystal structures of  $\text{Li}^+\cdot\text{FN}_2\text{O}_3$  and  $\text{Li}^+\cdot\text{HN}_2\text{O}_3$ , both with perchlorate counteranions. As can be seen in Figure 3 the differences in the coordination sphere of  $\text{Li}^+$  are striking. In Figure 3 both structure plots are viewed along the axis normal to the plane of the six-membered ring

(46) Wehrli, F. W.; Marchand, A. P.; Wehrli, S. *Interpretation of Carbon-13 NMR Spectra*; J. Wiley & Sons: New York, 1988.

(47) Harris, R. K.; Jackson, P. *Chem. Rev.* **1991**, *91*, 1427.

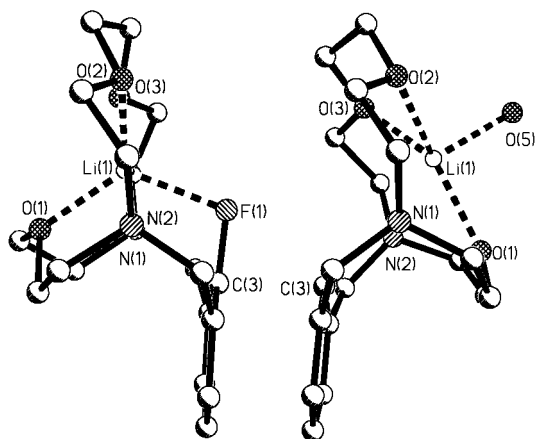


**Figure 4.** X-ray crystal structures of  $\text{FN}_2\text{O}_3 \cdot \text{Li}^+$  and  $\text{HN}_2\text{O}_3 \cdot \text{Li}^+$  (hydrogen atoms omitted).

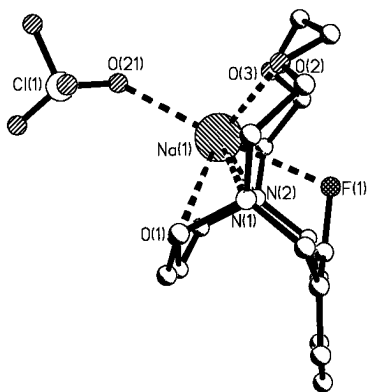


**Figure 5.** X-ray crystal structure of  $\text{FN}_2\text{O}_3 \cdot \text{Na}^+$  (hydrogen atoms omitted).

**Table 3.** Bond Lengths in the Coordination Spheres of  $\text{FN}_2\text{O}_3 \cdot \text{Li}^+$ ,  $\text{HN}_2\text{O}_3 \cdot \text{Li}^+$ , and  $\text{FN}_2\text{O}_3 \cdot \text{Na}^+$

	$\text{FN}_2\text{O}_3 \cdot \text{Li}^+$	$\text{HN}_2\text{O}_3 \cdot \text{Li}^+$	$\text{FN}_2\text{O}_3 \cdot \text{Na}^+$
$\text{M}^+ - \text{F}$ (pm)	203.5(5)		257.5(2)
$\text{M}^+ - \text{O}(1)$ (pm)	193.6(5)	200.5(5)	224.9(3)
$\text{M}^+ - \text{O}(2)$ (pm)	201.3(5)	215.0(5)	233.0(3)
$\text{M}^+ - \text{O}(3)$ (pm)	202.1(5)	210.2(5)	233.9(3)
$\text{M}^+ - \text{O}$ (pm)		192.8(6)	243.3(7)
$\text{M}^+ - \text{N}(1)$ (pm)	239.4(5)	277.1(7)	265.6(3)
$\text{M}^+ - \text{N}(2)$ (pm)	255.5(5)	273.4(7)	271.5(3)

and in Figure 4 parallel to the plane of the benzene ring. It can easily be seen in the two projections that  $\text{Li}^+$  is bonded symmetrically within the cavity of  $\text{FN}_2\text{O}_3$ , whereas this is not the case for  $\text{Li}^+ \cdot \text{HN}_2\text{O}_3$ . It becomes obvious that the fluorine atom in  $\text{Li}^+ \cdot \text{FN}_2\text{O}_3$  essentially behaves like an oxygen atom with respect to  $\text{Li}^+$ , since the distances of the four donor atoms to  $\text{Li}^+$  in its  $\text{O}_3\text{F}$  coordination sphere are rather similar (Table 3).

In the structure of  $\text{Li}^+ \cdot \text{HN}_2\text{O}_3$  the metal ion is moving away from the nitrogen atoms toward the edge of the cavity to contact an additional water molecule O(5). This results in an unusual trigonal-pyramidal  $\text{O}_4$  coordination, with the  $\text{Li}^+$ –nitrogen distances [277.1(7) and 273.4(7) pm] being much too long to be of significance (Table 3). It may be surprising that  $\text{Li}^+$  is leaving the center of the cavity to contact a water molecule despite the presence of two nitrogen atoms. However, it should be remembered that even in the structure of  $\text{Li}^+ \cdot \text{FN}_2\text{O}_3$  the  $\text{Li}^+$ –nitrogen distances are rather long and unsymmetrical [239.4(5) and 255.5(5) pm]. This is mainly due to the unfavorable geometric properties of the cryptand, since the two nitrogen atoms are fixed by the rigid *m*-xylyl bridge and cannot

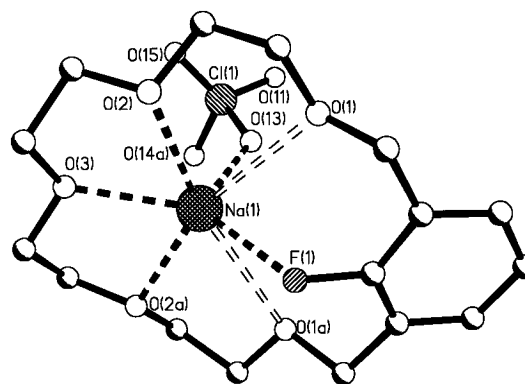


**Figure 6.** X-ray crystal structure of  $\text{FO}_5 \cdot \text{NaClO}_4$  (hydrogen atoms omitted).

approach each other close enough [ $\text{N}(1) - \text{N}(2) = 445.0$  pm in  $\text{Li}^+ \cdot \text{FN}_2\text{O}_3$  and 453.9 pm in  $\text{Li}^+ \cdot \text{HN}_2\text{O}_3$ ] to chelate a small metal ion such as  $\text{Li}^+$ .

The only explanation for the differences between the solid state structures of  $\text{Li}^+ \cdot \text{HN}_2\text{O}_3$  and  $\text{Li}^+ \cdot \text{FN}_2\text{O}_3$  must be the absence of the donor atom fluorine in the former ligand!

For the interpretation of the picrate extraction experiments described later it should be kept in mind that the presence of one additional water molecule coordinated to  $\text{Li}^+$  makes this solid state structure a good model for the species present in the water-saturated  $\text{CHCl}_3$  layer of the picrate extraction experiment.

A comparison of the solid state structures of  $\text{Li}^+ \cdot \text{FN}_2\text{O}_3$  with that of  $\text{FN}_2\text{O}_3$  eventually reveals a weakness of our hypothesis used to explain the shifts of the  $^{19}\text{F}$  NMR resonances. When calculating a rigid fit of the two molecules<sup>48</sup> by superimposing the respective benzene rings, it becomes apparent that the conformations of the two respective ether chains are not very different. In  $\text{Li}^+ \cdot \text{FN}_2\text{O}_3$  the O(1) is contacting the metal ion whereas it is bent away from this site in  $\text{FN}_2\text{O}_3$ . The chain between O(2) and O(3) is also slightly different in the complex and in the free ligand. Under the assumption that the solid state structures are reasonable models for the ensemble of structures present in solution, it is difficult to understand why addition of  $\text{Li}^+$  induces such large high-field shifts. However, the static picture obtained from the X-ray crystal structure does not provide information about the dynamics of the uncomplexed ligand in comparison with the rigidified oxyethylene chain upon metal coordination.

In  $\text{Na}^+ \cdot \text{FN}_2\text{O}_3$  (Figure 5) the much larger size of  $\text{Na}^+$  as compared to  $\text{Li}^+$  dictates that this ion is not located within the cavity but rather on the outside—which does not prevent the formation of fluorine–sodium contacts [ $\text{Na}^+ - \text{F} = 257.5(2)$  pm]. These distances are almost as short as typical sodium–oxygen distances in crown ether complexes<sup>49</sup> and are indicative of a significant interaction. Also remarkable in this structure are the rather short sodium–oxygen distances [224.9(3)–233.9(3) pm], giving the impression that sodium squeezes into the crown as much as possible to contact fluorine. Opposite to fluorine the nearly octahedral  $\text{FO}_5$  coordination sphere of sodium is completed by a monodentate perchlorate unit.

**2.3.3. Structures of  $\text{Na}^+ \cdot \text{FO}_5$  (Figure 6) and  $\text{Na}^+ \cdot \text{FNO}_4$  (Figure 7).** The sodium–fluorine distance of 237.4(5) pm in  $\text{Na}^+ \cdot \text{FO}_5$  is 20 pm shorter than in  $\text{Na}^+ \cdot \text{FN}_2\text{O}_3$  and is the second shortest bond in the coordination sphere of sodium (Table 4).

(48) *CHEM-X, Modelling Program*; Chemical Design Ltd.: Oxford, 1994.

(49) (a) Hilgenberger, R.; Saenger, W. In *Host Guest Complex Chemistry*; Vögtle, F., Weber, E., Eds.; Springer Verlag: Berlin, 1985; Chapter 2. (b) Dobler, M. *Ionophores and their Structures*; Wiley-Interscience: New York, 1981.

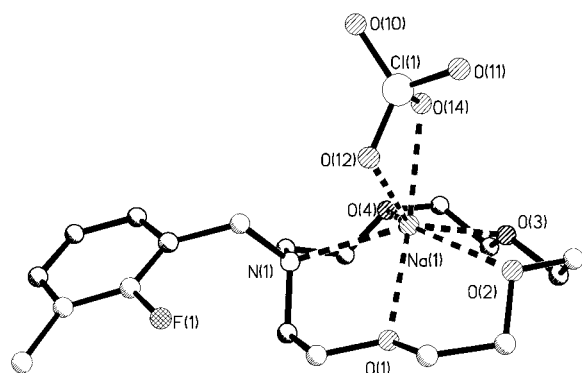


**Figure 7.** X-ray crystal structure of  $\text{FNO}_4 \cdot \text{NaClO}_4$  (hydrogen atoms omitted).

**Table 4.** Bond Lengths in the Coordination Spheres of  $\text{FO}_5 \cdot \text{Na}^+$ ,  $\text{FNO}_4 \cdot \text{Na}^+$ , and  $\text{FO}_5 \cdot \text{Ba}^{2+}$

	$\text{FO}_5 \cdot \text{Na}^+$	$\text{FNO}_4 \cdot \text{Na}^+$	$\text{FO}_5 \cdot \text{Ba}^{2+}$ 22
$\text{M}^+ - \text{F}$ (pm)	237.4(5)		279.9(8)
$\text{M}^+ - \text{O}(1)$ (pm)	302.0(3)	242.8(2)	279.4(5)
$\text{M}^+ - \text{O}(2)$ (pm)	257.4(3)	252.4(2)	279.5(5)
$\text{M}^+ - \text{O}(3)$ (pm)	240.2(5)	243.0(2)	
$\text{M}^+ - \text{O}(4)$ (pm)		242.8(2)	
$\text{M}^+ - \text{OCIO}_3$ (pm)	230.2(9)	257.7(3)	301.0(6)
$\text{M}^+ - \text{OCIO}_3$ (pm)		244.3(2)	281.0(7)
$\text{M}^+ - \text{N}(1)$ (pm)		260.8(2)	

Such large variations of bond length are quite normal in the coordination chemistry of the groups I and II metal ions and reflect the shallow potential curve for the binding of donor atoms. Quite like the nitrogen atoms in the cryptands the distance between O(1) and Na(1) [302.0(3) pm] is too long to account for a substantial interaction between these two atoms, but it is interesting that in the related complex of  $\text{Ba}(\text{ClO}_4)_2$  with  $\text{FO}_5$  the analogous barium–oxygen distance is much shorter [ $\text{Ba}^{2+} - \text{O} = 279.4(5)$  pm,  $\text{Ba}^{2+} - \text{F} = 279.9(8)$  pm].

In all structures described so far there is competition between perchlorate and the C–F unit for bonding to the metal ion, with the formation of close cation–anion pairs usually being disfavored. Starting from the cryptands  $\text{FN}_2\text{O}_3$  and  $\text{FN}_2\text{O}_4$  via the crown ethers  $\text{FO}_5$  and  $\text{FO}_6$  with a C–F bond pointing toward the center of the ring to the lariat type crown ether  $\text{FNO}_4$ , the degree of preorganization decreases, thus reducing the probability of close metal–fluorine contacts. The cavity of  $\text{FN}_2\text{O}_3$  is perfect for  $\text{Li}^+$  but is obviously too small for the sodium ion, resulting in participation of fluorine and perchlorate in the coordination sphere of  $\text{Na}^+$ , but not—as also appears possible—with a bidentate perchlorate substituting fluorine. The borderline between coordination of the C–F unit and the perchlorate group apparently is crossed in the crystal structure of  $\text{Na}^+ \cdot \text{FNO}_4$  in which the C–F unit is replaced by perchlorate in the coordination sphere of the metal ion. There is, however, very strong evidence from NMR experiments that fluorine–metal contacts are present in solution.

After the discussion of several solid state structures one question naturally arises: How long is a fluorine–metal ion  $\sigma$ -donor bond? Obviously we are not yet able to answer this question since it was only recently that Hay and Rustad gave a satisfactory answer for oxygen–metal ion  $\sigma$ -donor bonds.<sup>50</sup> The strain free  $r_o$  values for the modified MM3 force field as determined by Hay and Rustad for oxygen bonded to  $\text{Li}^+$ ,  $\text{Na}^+$ , and  $\text{Ba}^{2+}$  are 205, 238, and 283 pm, respectively, and provide an excellent guideline for us, since the covalent radii of oxygen

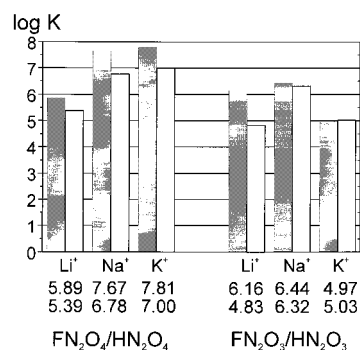


**Figure 8.** Bar diagram of the stability constants (F-cryptands shaded, H-cryptands white) as obtained from picrate extraction experiments. The stability constants ( $\log K$ ) are listed below the respective metal ions (upper value, F-cryptand; lower value, H-cryptand).

and fluorine are comparable. It is therefore significant to recall that we have observed slightly shorter metal–fluorine distances in the respective complexes of  $\text{Li}^+$ ,  $\text{Na}^+$ , and  $\text{Ba}^{2+}$  than the  $r_o$  values given by Hay and Rustad for metal–oxygen bonds.

**2.4. Stability Constants.** Metal–fluorine distances obtained from X-ray crystal structures as well as  $^{19}\text{F}$  NMR shifts  $\Delta\delta$  are not uniquely correlated with the strength of the metal–fluorine interaction. We therefore had to determine the stability constants of the complexes of fluoro macrocycles with different metal ions to evaluate the effect of fluorine coordination. The influence of the C–F unit on the binding of metal ions can be estimated when the stability constants of the fluoro macrocycles are compared with those of the respective fluorine free macrocycles. Pairs of closely related macrocycles which we have synthesized are  $\text{FN}_2\text{O}_3/\text{HN}_2\text{O}_3$ ,  $\text{FN}_2\text{O}_4/\text{HN}_2\text{O}_4$ ,  $\text{FO}_5/\text{HO}_5$ , and  $\text{FNO}_4/\text{HNO}_4$ .

**2.4.1. Picrate Extraction Experiments.** The stability of the complexes of  $\text{Li}^+$ ,  $\text{Na}^+$ , and  $\text{K}^+$  with the fluoro cryptands  $\text{FN}_2\text{O}_3/\text{HN}_2\text{O}_3$  and  $\text{FN}_2\text{O}_4/\text{HN}_2\text{O}_4$  were determined. In Figure 8 it is shown that the fluoro cryptands often form more stable complexes, but it is also apparent that a stabilizing effect of the C–F unit is not present in all complexes. This obviously reflects the fact that some metal ions fit into the cavity of the fluoro cryptands, whereas others are too big and hence cannot profit from contact with the C–F unit. The cavity size of  $\text{FN}_2\text{O}_3$  is ideal for  $\text{Li}^+$ , and that of  $\text{FN}_2\text{O}_4$  seems best suited for  $\text{Na}^+$  and  $\text{K}^+$ ; therefore, the differences in stability between the complexes of the fluorinated and the corresponding fluorine free ligand are largest. The difference in the stability constants of  $\text{Li}^+ \cdot \text{FN}_2\text{O}_3$  ( $K_{\text{ass-F}}$ ) and  $\text{Li}^+ \cdot \text{HN}_2\text{O}_3$  ( $K_{\text{ass-H}}$ ) amounts to  $\Delta G = 7.4$  kJ/mol. This value, however, must not be confused with the stabilization inferred by the F– $\text{Li}^+$   $\sigma$ -donor bond since the coordination spheres and the ligand geometries are quite different! It is very reasonable to assume that the solid state structure of  $\text{Li}^+ \cdot \text{HN}_2\text{O}_3$  involving the coordination of one additional water molecule to  $\text{Li}^+$  is a good model for the species present in the water-saturated  $\text{CHCl}_3$  layer of the picrate experiment. The enthalpic and entropic contributions of this additional water molecule and the different conformational energies of  $\text{FN}_2\text{O}_3$  and  $\text{HN}_2\text{O}_3$  will influence the overall stability constants as determined in the picrate experiment, thus blurring the effect produced by C–F coordination. It can be expected therefore that the stabilization inferred by fluorine coordination will be significantly larger.

At this point it is quite interesting to remember—as well as difficult to understand—that a spherand synthesized by Cram

(50) (a) Hay, B. P.; Rustad, J. R. *J. Am. Chem. Soc.* **1994**, *116*, 6316. (b) Hay, B. P. *Coord. Chem. Rev.* **1993**, *126*, 177.



et al. which has six fluorine atoms pointing toward the center of the cavity does not form stable complexes with group I metal ions.<sup>51</sup>

**2.4.2. NMR Competition Experiments.** The stability constants of the complexes of **FN<sub>2</sub>O<sub>4</sub>** and **HN<sub>2</sub>O<sub>4</sub>** with Li<sup>+</sup>, Na<sup>+</sup>, and K<sup>+</sup> are very high and close to the limit up to which picrate extraction experiments give reliable results as the picrate anion is extracted nearly quantitatively from the aqueous layer. Since we are less interested in absolute stabilities but more in the differences of the stability constants, we validated the values obtained in the picrate extraction by performing several NMR competition experiments. Equimolar mixtures of **FN<sub>2</sub>O<sub>4</sub>** and **HN<sub>2</sub>O<sub>4</sub>** were titrated with lithium, sodium, or potassium perchlorate while monitoring the characteristic shifts of the <sup>1</sup>H NMR resonance of the proton in the 2-position of the aromatic ring or the <sup>19</sup>F NMR resonances. The difference in the stability constant of the Li<sup>+</sup> complex of **FN<sub>2</sub>O<sub>4</sub>** and **HN<sub>2</sub>O<sub>4</sub>** thus obtained is  $K_F/K_H = 4$ , which compares well with the corresponding value from the extraction experiment ( $K_{\text{ass-F}}/K_{\text{ass-H}} = 3.7$ ). Unfortunately the NMR competition experiment was rendered almost useless in the case of the Na<sup>+</sup> and K<sup>+</sup> complexes due to severe line broadening. In a rough estimate it could only be concluded that the differences obtained in the picrate experiment are qualitatively correct.

The same technique was applied for the Na<sup>+</sup> complexes of the lariat type crown ethers **FNO<sub>4</sub>** and **HNO<sub>4</sub>**, revealing a very small stabilization of 7% for the fluorine-containing macrocycle. A more significant stabilization of ca. 50% has been reported for the Na<sup>+</sup> complex of **FO<sub>5</sub>** versus that of **HO<sub>5</sub>**.<sup>22</sup> It would thus be interesting to see if the analogous compounds **ClO<sub>5</sub>** and **BrO<sub>5</sub>**<sup>52</sup> gave a similar stabilization with respect to **HO<sub>5</sub>** or if the steric bulk of the larger halides prevented complex formation.

### 3. Conclusions

The results reported here provide conclusive evidence for the concept in which C–F groups are regarded as efficient donor units for groups I and II metal ions, just as predicted by Glusker et al. in 1983.<sup>9,53</sup>

This was proven by determining the heterogeneous stability constants of the complexes of group I metal ions with fluoro macrocycles and with the analogous fluorine free macrocycles. Metal complexes of the fluoro macrocycles are more stable than those of the analogous fluorine free macrocycles, as long as the metal ion is small enough to migrate into the cavity to contact fluorine. The stabilizing effect of a fluorine–metal  $\sigma$ -donor bond is thus most pronounced in Li<sup>+</sup>·**FN<sub>2</sub>O<sub>3</sub>**, Na<sup>+</sup>·**FN<sub>2</sub>O<sub>4</sub>**, and K<sup>+</sup>·**FN<sub>2</sub>O<sub>4</sub>** as compared with the related complexes of **HN<sub>2</sub>O<sub>3</sub>** and **HN<sub>2</sub>O<sub>4</sub>**. However, just like in conventional macrocycles the stable complexation of group I metal ions through C–F contacts in fluoro macrocycles requires a sufficient degree of preorganization to be built into the ligand; therefore, the relative stabilization due to fluorine coordination decreases in the order fluoro cryptand > fluoro crown ether > fluoro lariat crown ether.

The complexation of groups I and II metal ions by fluoro macrocycles leads to shifts of the <sup>19</sup>F NMR resonances (relative to the respective free ligands) of between  $\Delta\delta = -18.2$  ppm

and  $\Delta\delta = +8.5$  ppm. Especially the complexes of **FN<sub>2</sub>O<sub>3</sub>** and **FN<sub>2</sub>O<sub>4</sub>** are characterized by large high-field shifts of the <sup>19</sup>F NMR resonances upon metal complexation. A qualitative model has been presented which attempts to rationalize the shifts of the NMR resonances. Accordingly two effects are responsible for the shifts of the NMR signals: a shielding influence of the oxyethylene chain and a deshielding influence of the metal cations. In the conformationally restricted fluoro cryptands the shielding effect is dominating, resulting in large negative  $\Delta\delta$  values. The longer and thus the more flexible the oxyethylene chain the smaller its shielding contribution and the more important the positive charge of the metal ions becomes. In Ca<sup>2+</sup>·**FO<sub>5</sub>** and Sr<sup>2+</sup>·**FO<sub>5</sub>** both counteracting effects are equal—but of opposite sign—resulting in  $\Delta\delta \approx 0$ , whereas  $\Delta\delta$  is positive for Ba<sup>2+</sup>·**FO<sub>5</sub>** as well as in most metal complexes of **FO<sub>6</sub>**, **F(NO<sub>3</sub>)<sub>2</sub>**, **F(NO<sub>4</sub>)<sub>2</sub>**, and **F(NO<sub>5</sub>)<sub>2</sub>**. To estimate the strength of metal–fluorine interactions in solution the <sup>1</sup>J<sub>CF</sub> coupling constants seem to be a reliable guide as they are decreased by up to 23 Hz upon metal coordination relative to the free ligands.

Several solid state structures of fluoro macrocycle metal complexes demonstrate that fluorine and oxygen are equal partners in the coordination sphere of the respective metal ion, as evidenced by similar metal–fluorine and metal–oxygen distances. The comparison of the structures of Li<sup>+</sup>·**FN<sub>2</sub>O<sub>3</sub>** and Li<sup>+</sup>·**HN<sub>2</sub>O<sub>3</sub>**·H<sub>2</sub>O reveals different Li<sup>+</sup>-coordination spheres (O<sub>3</sub>F vs O<sub>4</sub>) and a different spatial arrangement of the donor atoms in these two complexes, stressing once more the importance of fluorine coordination.

Finally it should be noted that <sup>19</sup>F NMR spectroscopical investigations of metal complexes with fluoro macrocycles will be a powerful tool in the hands of those interested in coordination chemistry. Such studies should lead to a much better understanding of the behavior of metal ions in solution, which currently lags far behind the knowledge accumulated in the course of numerous X-ray crystal structure determinations.

### 5. Experimental Section

**5.1. General Procedures.** Commercially available solvents and reagents were purified according to literature procedures. Chromatography was carried out with silica MN 60. NMR spectra were recorded at 300 K with a Bruker AC200 F (<sup>1</sup>H NMR, 200 MHz; <sup>13</sup>C NMR, 50.3, MHz; <sup>19</sup>F NMR, 188.2 MHz; <sup>23</sup>Na, 52.9 MHz) or a Varian Unity 300 (<sup>1</sup>H NMR, 300 MHz; <sup>6</sup>Li, 44.1 MHz; <sup>7</sup>Li, 116.6 MHz; <sup>13</sup>C NMR, 75.4 MHz). <sup>1</sup>H NMR spectra were referenced to residual H impurities in the solvent and <sup>13</sup>C NMR spectra to the respective solvent signals: CDCl<sub>3</sub> (7.26 and 77.0 ppm) and CD<sub>3</sub>CN (1.93 and 1.30 ppm). <sup>13</sup>C NMR spectra were accumulated in 32K data fields in both the time and frequency domains with a digital resolution of 0.8 Hz/point. <sup>19</sup>F NMR spectra were referenced to internal CFC<sub>3</sub> (0 ppm). Solid state MAS NMR spectra were recorded on a Bruker ASX 500 at 470.6 MHz (rotation 15 kHz) and were referenced externally against PTFE, –123.2 ppm. Elemental analyses were performed at the Mikroanalytisches Laboratorium der Chemischen Laboratorien Universität Freiburg. Melting points were determined with a Meltemp melting point apparatus in sealed capillaries. Starting materials were available commercially or prepared according to literature procedures: 1,3-dimethyl-2-fluorobenzene,<sup>54</sup> 1,3-bis(bromomethyl)-2-fluorobenzene,<sup>23</sup> **HO<sub>5</sub>**,<sup>25</sup> diaza-18-crown-6,<sup>55</sup> aza-12-crown-4,<sup>56</sup> aza-15-crown-5 and aza-18-crown-6,<sup>57</sup> triflate salts,<sup>58</sup> and picrate salts.<sup>59</sup> Picrate extraction experiments were

(54) Plenio, H.; Diodone, R. *Z. Naturforsch.* **1995**, *50b*, 1075.

(55) (a) Kulstad, S.; Malmsten, L. A. *Acta Chem. Scand., Ser. B* **1979**, *33*, 469. (b) Kulstad, S.; Malmsten, L. A. *Tetrahedron Lett.* **1980**, *21*, 643.

(56) Calverly, M. J.; Dale, J. *Acta Chem. Scand., Ser. B* **1982**, *36*, 241.

(57) Maeda, H.; Furuyoshi, S.; Nakatsuji, Y.; Okahara, M. *Bull. Chem. Soc. Jpn.* **1983**, *56*, 212.

(58) Dixon, N. E.; Lawrance, G. A.; Lay, P. A.; Sargeson, A. M.; Taube, H. *Inorg. Synth.* **1990**, *28*, 70 (Angelici, R. J., Ed.).

(59) (a) Copland, M. A.; Fuoss, R. M. *J. Phys. Chem.* **1964**, *68*, 1177. (b) Brown, R.; Jones, W. E. *J. Chem. Soc.* **1946**, 781.

(51) Paek, K.; Knobler, C. B.; Maverick, E. F.; Cram, D. J. *J. Am. Chem. Soc.* **1989**, *111*, 8662.

(52) (a) Skowronska-Ptasinka, M.; Aarts, V. M. L. J.; Egerbrink, R. J. M.; vanEerden, J.; Harkema, J.; Reinhoudt, D. N. *J. Org. Chem.* **1988**, *53*, 5484. (b) Markies, P. R.; Villena, A.; Akkerman, O. S.; Bickelhaupt, F.; Smets, W. J. J.; Spek, A. L. *J. Organomet. Chem.* **1993**, *463*, 7.

(53) This prediction also seems to hold true for H<sup>+</sup> coordination: Plenio, H.; Diodone, R. To be published.

carried out according to a procedure by Cram et al. and were performed under the same conditions used to reproduce the literature values for dicyclohexano-18-crown-6.<sup>60</sup>

**4,7,20-Trioxa-1,10-diazatricyclo[8.7.5.1<sup>12,16</sup>]tricoso-12,14,16(23)-triene (HN<sub>2</sub>O<sub>3</sub>).** A mixture of 1,4,10-trioxa-7,13-diazacyclopentadecane (400 mg, 1.88 mmol), 1,3-bis(bromomethyl)benzene (500 mg, 1.88 mmol), and Na<sub>2</sub>CO<sub>3</sub> (3.3 g) in acetonitrile (120 mL) was refluxed for 16 h. The mixture was filtered and washed with acetonitrile (25 mL) and the solvent evaporated *in vacuo*. The residue was subjected to silica gel column chromatography with cyclohexane–diethylamine (5:1) to give HN<sub>2</sub>O<sub>3</sub> as a solid. Recrystallization from PE 60/70 yielded HN<sub>2</sub>O<sub>3</sub> (280 mg, 0.88 mmol, 47%) as a colorless solid. HN<sub>2</sub>O<sub>3</sub>: mp 62–64 °C; <sup>1</sup>H NMR (CD<sub>3</sub>CN)  $\delta$  2.34–2.46 (2H, ddd,  $J = 1.9$  Hz, 7.0 Hz, 14.1 Hz), 2.60–2.71 (2H, ddd,  $J = 2.1$  Hz, 6.3 Hz, 14.1 Hz), 2.79–2.90 (6H, m), 3.26–3.36 (2H, m), 3.43–3.79 (10H, m), 3.97 (2H, d,  $J = 15.6$  Hz, ArCH<sub>2</sub>), 6.87–7.09 (3H, m, ArH), 8.86 (1H, s, ArH); <sup>13</sup>C NMR (CD<sub>3</sub>CN)  $\delta$  57.73, 59.10, 60.40, 70.40 (CO), 70.48 (CO), 70.84 (CO), 124.91 (Ar), 124.28 (Ar), 132.58 (Ar), 142.87 (Ar). HN<sub>2</sub>O<sub>3</sub>·LiClO<sub>4</sub>: mp 104 °C; <sup>1</sup>H NMR (CD<sub>3</sub>CN)  $\delta$  2.14–2.23 (2H, m), 2.41–2.67 (4H, m), 2.73–3.00 (4H, m), 3.12–3.22 (2H, m), 3.29 (2H, d,  $J = 13.5$  Hz, ArCH<sub>2</sub>), 3.59–3.87 (8H, m), 4.08 (2H, d,  $J = 13.5$  Hz, ArCH<sub>2</sub>), 7.12–7.28 (3H, m, ArH), 7.47 (1H, s, ArH); <sup>13</sup>C NMR (CD<sub>3</sub>CN)  $\delta$  54.12, 57.08, 60.84, 68.04 (CO), 68.63 (CO), 69.35 (CO), 127.74 (Ar), 129.29 (Ar), 131.78 (Ar), 142.74 (Ar). HN<sub>2</sub>O<sub>3</sub>·NaClO<sub>4</sub>: <sup>1</sup>H NMR (CD<sub>3</sub>CN)  $\delta$  2.66 (2H, d,  $J = 14$  Hz), 2.80–2.86 (4H, m), 2.92 (2H, m), 3.06–3.11 (2H, m), 3.18 (2H, d,  $J = 15.3$  Hz, ArCH<sub>2</sub>), 3.61–3.83 (10H, m), 4.16 (2H, d,  $J = 15.3$  Hz, ArCH<sub>2</sub>), 7.04–7.18 (2H, m, ArH), 7.63 (1H, s, ArH). HN<sub>2</sub>O<sub>3</sub>·KSO<sub>3</sub>CF<sub>3</sub>: <sup>1</sup>H NMR (CD<sub>3</sub>CN)  $\delta$  2.62 (2H, d,  $J = 14$  Hz), 2.80–2.85 (4H, m), 2.91–3.05 (5H, m), 3.19 (2H, d,  $J = 16.4$  Hz, ArCH<sub>2</sub>), 3.50–3.72 (9H, m), 4.11 (2H, d,  $J = 16.6$  Hz, ArCH<sub>2</sub>), 6.95 (2H, m, ArH), 7.09–7.18 (1H, m), 8.46 (1H, s, ArH).

**23-Fluoro-4,7,20-trioxa-1,10-diazatricyclo[8.7.5.1<sup>12,16</sup>]tricoso-12,14,16(23)-triene (FN<sub>2</sub>O<sub>3</sub>).** A mixture of 1,4,10-trioxa-7,13-diazacyclopentadecane (400 mg, 1.88 mmol), 1,3-bis(bromomethyl)-2-fluorobenzene (530 mg, 1.88 mmol), and Na<sub>2</sub>CO<sub>3</sub> (3.3 g) in acetonitrile (120 mL) was refluxed for 16 h. The mixture was filtered and washed with acetonitrile (25 mL) and the solvent evaporated *in vacuo*. The residue was subjected to silica gel column chromatography with cyclohexane–diethylamine (5:1) to give FN<sub>2</sub>O<sub>3</sub> as a solid. Recrystallization from PE 60/70 yielded FN<sub>2</sub>O<sub>3</sub> (320 mg, 51%) as a colorless solid. Single crystals of FN<sub>2</sub>O<sub>3</sub> were obtained by recrystallization from 2-propanol. FN<sub>2</sub>O<sub>3</sub>: mp 62–64 °C; <sup>1</sup>H NMR (CD<sub>3</sub>CN)  $\delta$  2.30–2.34 (4H, m, NCH<sub>2</sub>), 2.50–2.63 (2H, ddd,  $J = 14.4$  Hz, 9.1 Hz, 2.1 Hz, NCH), 2.84 (1H, t,  $J = 2.2$  Hz, OCH), 2.88 (1H, t,  $J = 2.2$  Hz, OCH<sub>2</sub>), 2.94–3.05 (2H, ddd,  $J = 14.3$ , 4.1, 1.8 Hz, OCH<sub>2</sub>), 3.11–3.22 (2H, m, OCH<sub>2</sub>), 3.25–3.35 (4H, m, ArCH<sub>2</sub>, NCH<sub>2</sub>), 3.57–3.76 (6H, m, OCH<sub>2</sub>, OCH<sub>2</sub>), 4.00 (2H, d,  $J = 12.5$  Hz, ArCH<sub>2</sub>), 6.79–6.87 (1H, m, ArH), 6.97–7.04 (2H, m, ArH); <sup>13</sup>C NMR (CD<sub>3</sub>CN)  $\delta$  54.94, 56.18, 59.42, 70.11, 70.39 (d,  $J_{CF} = 1.5$  Hz), 71.61, 130.17, 130.35 (d,  $J_{CF} = 5.5$  Hz), 164.39 (d,  $J_{CF} = 256$  Hz). FN<sub>2</sub>O<sub>3</sub>·LiClO<sub>4</sub>: mp 168 °C; <sup>1</sup>H NMR (CD<sub>3</sub>CN)  $\delta$  2.31–2.48 (6H, m, NCH<sub>2</sub>, OCH<sub>2</sub>), 2.78–3.00 (4H, ddd,  $J = 14.0$  Hz, 6.8 Hz, 6.0 Hz, 3.6 Hz, NCH<sub>2</sub>), 3.31–3.28 (2H, m, OCH<sub>2</sub>), 3.44 (2H, dd,  $J = 12.9$  Hz, 2.2 Hz, ArCH), 3.55–3.61 (2H, m, OCH<sub>2</sub>), 3.69–3.80 (6H, m, OCH<sub>2</sub>), 7.14–7.22 (1H, m, ArH), 7.28–7.35 (2H, m, ArH); <sup>13</sup>C NMR (CD<sub>3</sub>CN)  $\delta$  51.65 (CN), 56.62 (CN), 57.29 (ArCH<sub>2</sub>), 67.53 (CO), 68.51 (CO), 69.30 (CO), 126.23 (d,  $J_{CF} = 3$  Hz, C4), 130.55 (d,  $J_{CH} = 11$  Hz, C2), 131.22 (d,  $J_{CF} = 6.5$  Hz, C3), 162.37 (d,  $J_{CF} = 238.5$  Hz, C1). FN<sub>2</sub>O<sub>3</sub>·<sup>6</sup>LiClO<sub>4</sub>: <sup>6</sup>Li NMR (CD<sub>3</sub>CN)  $\delta$  1.58 (d,  $J_{LiF} = 7.8$  Hz); <sup>19</sup>F NMR (CD<sub>3</sub>CN)  $\delta$  -127.2 (t,  $J_{LiF} = 7.6$  Hz). FN<sub>2</sub>O<sub>3</sub>·<sup>7</sup>LiClO<sub>4</sub>: <sup>7</sup>Li NMR (CD<sub>3</sub>CN)  $\delta$  0.29 (d,  $J_{LiF} = 19.0$  Hz); <sup>19</sup>F NMR (CD<sub>3</sub>CN)  $\delta$  -127.3 (q,  $J_{LiF} = 19$  Hz). FN<sub>2</sub>O<sub>3</sub>·NaClO<sub>4</sub>: mp 257 °C; <sup>1</sup>H NMR (CD<sub>3</sub>CN)  $\delta$  1.94–2.06 (2H, m), 2.63–3.11 (10H, m), 3.20 (2H, dd,  $J = 14.5$ , 2.3 Hz, ArCH<sub>2</sub>), 3.56 (1H, t,  $J = 2.2$  Hz), 3.61 (1H, t,  $J = 2.2$  Hz), 3.71–3.98 (6H, m), 4.30 (2H, d,  $J = 14.4$  Hz, ArCH<sub>2</sub>), 6.96–7.03 (1H, m, ArH), 7.22–7.30 (2H, m, ArH); <sup>13</sup>C NMR (CD<sub>3</sub>CN)  $\delta$  56.25, 60.31 (d,  $J_{CF} = 1.2$  Hz), 60.57, 69.19, 69.49 (d,  $J_{CF} = 2.0$  Hz), 69.65, 124.48 (d,  $J_{CF} = 4.0$  Hz, Ar), 129.84 (d,  $J_{CF} = 5.5$  Hz, Ar), 130.12 (d,  $J_{CF} = 11$  Hz, Ar),

162.35 (d,  $J_{CF} = 246.5$  Hz, Ar); <sup>19</sup>F NMR (CD<sub>3</sub>CN)  $\delta$  -114.26 (s); <sup>23</sup>Na NMR (CD<sub>3</sub>CN)  $\delta$  6.0 (s,  $\nu_{1/2} = 205$  Hz). FN<sub>2</sub>O<sub>3</sub>·KSO<sub>3</sub>CF<sub>3</sub>: <sup>1</sup>H NMR (CD<sub>3</sub>CN)  $\delta$  2.06–2.18 (2H, m), 2.53–2.87 (8H, m), 2.97–3.04 (2H, m), 3.15 (2H, dd,  $J = 14.0$ , 2.3 Hz, ArCH<sub>2</sub>), 3.44 (1H, t,  $J = 2.3$  Hz), 3.49 (1H, t,  $J = 2.2$  Hz), 3.70 (4H, d,  $J = 1.4$  Hz), 3.82–3.93 (2H, m), 4.20 (2H, d,  $J = 13.8$  Hz, ArCH<sub>2</sub>), 6.83–6.90 (1H, m, ArH), 7.09–7.16 (2H, m, ArH); <sup>13</sup>C NMR (CD<sub>3</sub>CN)  $\delta$  56.55 (d,  $J_{CF} = 1.4$  Hz, ArCH<sub>2</sub>), 59.12 (CN), 59.87 (CN), 69.60 (CO), 69.88 (CO), 70.41 (CO), 122.83 (d,  $J_{CF} = 4$  Hz, Ar), 129.26 (d,  $J_{CF} = 5.5$  Hz, Ar), 130.38 (d,  $J_{CF} = 12.0$  Hz, Ar), 163.34 (d,  $J_{CF} = 257$  Hz, Ar). FN<sub>2</sub>O<sub>3</sub>·Ca(ClO<sub>4</sub>)<sub>2</sub>: <sup>1</sup>H NMR (CD<sub>3</sub>CN)  $\delta$  2.15–2.26 (2H, m), 2.70 (s), 2.83 (4H, d,  $J = 14$  Hz), 3.25–3.45 (m), 3.91–4.29 (m), 4.52 (d,  $J = 14$  Hz), 7.13–7.21 (1H, m), 7.37–7.45 (1H, m); <sup>13</sup>C NMR (CD<sub>3</sub>CN)  $\delta$  56.31, 57.24, 58.06, 70.47, 70.49, 71.09, 72.14, 126.41 (d,  $J_{CF} = 4$  Hz), 128.60 (d,  $J_{CF} = 10$  Hz), 130.46 (d,  $J_{CF} = 5.5$  Hz), 161.49 (d,  $J_{CF} = 239$  Hz).

**4,7,13,16-Tetraoxa-1,10-diazatricyclo[8.8.7.1<sup>20,24</sup>]hexacoso-20,22,24(26)-triene (HN<sub>2</sub>O<sub>4</sub>).** A mixture of 1,4,10,13,16-tetraoxa-7,13-diazacyclooctadecane (1.5 g, 5.7 mmol), 1,3-bis(bromomethyl)benzene (1.5 g, 5.7 mmol) and K<sub>2</sub>CO<sub>3</sub> (3 g) in acetonitrile (250 mL) was refluxed for 18 h. The mixture was filtered and washed with acetonitrile (25 mL) and the solvent evaporated *in vacuo*. The residue was subjected to silica gel column chromatography with cyclohexane–diethylamine (5:1) to give HN<sub>2</sub>O<sub>4</sub> as a solid. Recrystallization from PE 60/70 yielded HN<sub>2</sub>O<sub>4</sub> (580 mg, 1.6 mmol, 28%) as a colorless solid. HN<sub>2</sub>O<sub>4</sub>: mp 96 °C; <sup>1</sup>H NMR (CDCl<sub>3</sub>)  $\delta$  2.61–2.81 (8H, m, NCH<sub>2</sub>), 3.44–3.76 (20H, m, ArCH<sub>2</sub>, OCH<sub>2</sub>), 6.91–7.18 (3H, m, ArH), 8.41 (1H, s, ArH); <sup>13</sup>C NMR (CDCl<sub>3</sub>)  $\delta$  55.92, 59.40, 69.38 (CO), 70.27 (CO), 125.10 (Ar), 126.71 (Ar), 129.42 (Ar), 141.54 (Ar).

**26-Fluoro-4,7,13,16-tetraoxa-1,10-diazatricyclo[8.8.7.1<sup>20,24</sup>]hexacoso-20,22,24(26)-triene (FN<sub>2</sub>O<sub>4</sub>) and 35,44-Difluoro-6,9,23,26,38,41,47,50-octa-3,12,20,29-tetraazapentacyclo[29.8<sup>3,12,3,20,29</sup>.3<sup>1,31</sup>.1<sup>31,1</sup>.1<sup>4,18</sup>]dopentaconta-14,16,18(44),31,33,1(35)-hexene ((FN<sub>2</sub>O<sub>4</sub>)<sub>2</sub>).** A mixture of 1,4,10,13,16-tetraoxa-7,13-diazacyclooctadecane (1.5 g, 5.7 mmol), 1,3-bis(bromomethyl)-2-fluorobenzene (1.6 g, 5.7 mmol), KBr (1.0 g), and K<sub>2</sub>CO<sub>3</sub> (3 g) in acetonitrile (250 mL) was refluxed for 18 h. The mixture was filtered and washed with acetonitrile (25 mL) and the solvent evaporated *in vacuo*. The residue was subjected to silica gel column chromatography with cyclohexane–diethylamine (5:1) to give FN<sub>2</sub>O<sub>4</sub> and (FN<sub>2</sub>O<sub>4</sub>)<sub>2</sub> as colorless solids. Recrystallization from PE 60/70 yielded FN<sub>2</sub>O<sub>4</sub> (0.74 g, 1.9 mmol, 34%). (FN<sub>2</sub>O<sub>4</sub>)<sub>2</sub> was recrystallized from toluene (0.92 g, 1.2 mmol, 21%). FN<sub>2</sub>O<sub>4</sub>: mp 96 °C; <sup>1</sup>H NMR (CD<sub>3</sub>CN)  $\delta$  2.52–2.72 (8H, m, NCH<sub>2</sub>), 3.25–3.67 (20H, m, OCH<sub>2</sub>, ArCH<sub>2</sub>), 6.91–6.99 (1H, m, ArH), 7.09–7.16 (2H, m, ArH); <sup>13</sup>C NMR (CD<sub>3</sub>CN)  $\delta$  55.45 (d,  $J_{CF} = 1.5$  Hz, ArCH<sub>2</sub>), 57.04 (CN), 69.27 (CO), 71.18 (d,  $J_{CF} = 1.5$  Hz, CO), 122.88 (d,  $J_{CF} = 4.0$  Hz, Ar), 129.34 (d,  $J_{CF} = 14.4$  Hz, Ar), 130.60 (d,  $J_{CF} = 4.8$  Hz, Ar), 162.67 (d,  $J_{CF} = 252$  Hz, Ar); <sup>13</sup>C NMR (CDCl<sub>3</sub>)  $\delta$  55.31, 56.43, 68.69 (CO), 70.42 (CO), 122.08 (d, 4.5 Hz, Ar), 128.14 (d,  $J_{CF} = 13.5$  Hz, Ar), 129.61 (d,  $J_{CF} = 5$  Hz, Ar), 161.64 (d,  $J_{CF} = 253$  Hz, Ar); <sup>19</sup>F NMR (CD<sub>3</sub>CN)  $\delta$  -114.38; MS  $m/z$  382 (M<sup>+</sup>). FN<sub>2</sub>O<sub>4</sub>·LiClO<sub>4</sub>: <sup>1</sup>H NMR (CD<sub>3</sub>CN)  $\delta$  2.55–2.77 (8H, m, NCH<sub>2</sub>), 3.47–3.71 (20H, m, OCH<sub>2</sub>, ArCH<sub>2</sub>), 7.08–7.15 (1H, m, ArH), 7.21–7.28 (2H, m, ArH); <sup>13</sup>C NMR (CD<sub>3</sub>CN)  $\delta$  54.08, 55.58, 68.83, 69.83, 125.32 (d,  $J_{CF} = 4$  Hz, Ar), 129.45 (d,  $J_{CF} = 11$  Hz, Ar), 130.97 (d,  $J_{CF} = 5.5$  Hz, Ar), 161.55 (d,  $J_{CF} = 238.5$  Hz, Ar); <sup>19</sup>F NMR (CD<sub>3</sub>CN)  $\delta$  -127.17 (s). FN<sub>2</sub>O<sub>4</sub>·NaClO<sub>4</sub>: <sup>1</sup>H NMR (CD<sub>3</sub>CN, 340 K)  $\delta$  2.67 (8H, s,  $\nu_{1/2} = 11.5$  Hz, NCH<sub>2</sub>), 3.4–3.6 (20H, br,  $\nu_{1/2} = 50$  Hz, ArCH<sub>2</sub>, OCH<sub>2</sub>), 7.09–7.17 (1H, m, ArH), 7.23–7.30 (2H, m, ArH); <sup>13</sup>C NMR (CD<sub>3</sub>CN)  $\delta$  54.30 (d,  $J_{CF} = 1.6$  Hz, ArCH<sub>2</sub>), 67.74 (br), 69.54, 124.90 (d,  $J_{CF} = 5$  Hz, Ar), 129.16 (d,  $J_{CF} = 13$  Hz, Ar), 131.22 (d,  $J_{CF} = 5$  Hz, Ar), 161.00 (d,  $J_{CF} = 242.5$  Hz, Ar); <sup>19</sup>F NMR (CD<sub>3</sub>CN)  $\delta$  -125.36 (t,  $J = 8.3$  Hz); <sup>23</sup>Na NMR (CD<sub>3</sub>CN)  $\delta$  -9.1 (s,  $\nu_{1/2} = 224$  Hz). FN<sub>2</sub>O<sub>4</sub>·KSO<sub>3</sub>CF<sub>3</sub>: <sup>1</sup>H NMR (CD<sub>3</sub>CN)  $\delta$  2.66–2.88 (8H, m, NCH<sub>2</sub>), 3.28–3.70 (20H, m, br, OCH<sub>2</sub>, ArCH<sub>2</sub>), 7.01–7.08 (1H, m, ArH), 7.24–7.32 (2H, m, ArH); <sup>13</sup>C NMR (CD<sub>3</sub>CN)  $\delta$  55.17, 60.41 (br), 68.50 (d,  $J_{CF} = 1.6$  Hz), 69.31, 124.49 (d,  $J_{CF} = 4$  Hz, Ar), 130.06 (d,  $J_{CF} = 14$  Hz, Ar), 130.80 (d,  $J_{CF} = 5.5$  Hz, Ar), 161.41 (d,  $J_{CF} = 246.5$  Hz, Ar); <sup>19</sup>F NMR (CD<sub>3</sub>CN)  $\delta$  -118.9 (s). FN<sub>2</sub>O<sub>4</sub>·RbSO<sub>3</sub>CF<sub>3</sub>: <sup>1</sup>H NMR (CD<sub>3</sub>CN, 325 K)  $\delta$  2.61–2.70 (5H, m), 2.79–2.92 (5H, m), 3.16 (4H, s, br), 3.27 (2H, t,  $J = 2.8$  Hz), 3.32 (2H, t,  $J = 2.8$  Hz), 3.40–3.49 (4H, m), 3.58 (3H, s), 3.79 (3H, t,  $J = 10.7$  Hz), 6.99–7.06 (1H, m,

(60) (a) Moore, S. S.; Tarnowski, T. L.; Newcomb, M.; Cram, D. J. *J. Am. Chem. Soc.* **1977**, *99*, 6398. (b) Koenig, K. E.; Lein, G. M.; Stuckler, P.; Kaneda, T.; Cram, D. J. *J. Am. Chem. Soc.* **1979**, *101*, 3553.

**Table 5.** X-ray Crystal Structure Data Summary

	<b>FN<sub>2</sub>O<sub>3</sub></b>	<b>FN<sub>2</sub>O<sub>3</sub>·Li<sup>+</sup></b>	<b>HN<sub>2</sub>O<sub>3</sub>·Li<sup>+</sup></b>	<b>FN<sub>2</sub>O<sub>3</sub>·Na<sup>+</sup></b>	<b>FO<sub>5</sub>·Na<sup>+</sup></b>	<b>FNO<sub>4</sub>·Na<sup>+</sup></b>
empirical formula	C <sub>18</sub> H <sub>27</sub> FN <sub>2</sub> O <sub>3</sub>	C <sub>18</sub> H <sub>27</sub> ClFLiN <sub>2</sub> O <sub>7</sub>	C <sub>18</sub> H <sub>28</sub> ClLiN <sub>2</sub> O <sub>7</sub>	C <sub>18</sub> H <sub>27</sub> ClFN <sub>2</sub> NaO <sub>7</sub>	C <sub>16</sub> H <sub>25</sub> ClFN <sub>2</sub> NaO <sub>9</sub>	C <sub>18</sub> H <sub>28</sub> ClFNNaO <sub>8</sub>
formula weight (g mol <sup>-1</sup> )	338.42	444.81	426.81	460.86	436.78	463.85
temperature (K)	293(2)	293(2)	293(2)	293(2)	293(2)	293(2)
crystal system	orthorhombic	monoclinic	monoclinic	orthorhombic	orthorhombic	monoclinic
space group	<i>Pbca</i>	<i>P2<sub>1</sub>/c</i>	<i>P2<sub>1</sub>/n</i>	<i>Pbca</i>	<i>Pmn2<sub>1</sub></i>	<i>P2<sub>1</sub>/c</i>
unit cell dimensions (pm or deg)						
a	8.522(2)	7.822(2)	13.131(3)	14.284(3)	11.213(2)	9.580(2)
b	15.121(3)	22.790(5)	11.265(2)	14.472(3)	10.931(2)	27.882(6)
c	28.102(6)	12.024(2)	15.043(3)	20.528(4)	8.091(2)	9.439(2)
α	90	90	90	90	90	90
β	90	98.96(3)	101.39(3)	90	90	118.38(3)
γ	90	90	90	90	90	90
volume (Å <sup>3</sup> )	3621.3(14)	2117.3(8)	2181.3(8)	4244(2)	991.7(4)	2218.2(8)
Z	8	4	4	8	2	4
density (g cm <sup>-3</sup> )	1.241	1.395	1.300	1.443	1.463	1.389
absorption (mm <sup>-1</sup> )	0.091	0.231	0.215	0.252	0.270	0.243
<i>F</i> (000)	1456	936	904	1936	456	976
crystal size (mm)	0.6 × 0.5 × 0.5	0.6 × 0.4 × 0.4	0.6 × 0.6 × 0.4	0.4 × 0.3 × 0.3	0.6 × 0.2 × 0.15	0.5 × 0.5 × 0.15
θ range (deg)	2.7–23.5	2.8–26.3	2.3–26.3	2.4–24.9	2.6–26.0	2.4–26.0
index range ( <i>hkl</i> )	−9/0, −16/0, −31/0	−9/9, 0/28, −14/0	−16/16, −14/0, −18/0	−16/0, −17/0, 0/24	−13/0, −13/0, 0/9	−11/10, 0/34, 0/11
reflections (collected, independent)	2663, 2662	4491, 4287	4596, 4426	3680, 3680	1101, 1101	4619/4349
no. of data/no. of parameters	2277/218	3516/303	3727/326	2721/300	930/154	3551/282
Goof	1.040	1.065	1.06	1.08	1.064	1.073
final <i>R</i> indices [ <i>I</i> > 2σ( <i>I</i> )] ( <i>R</i> <sub>1</sub> , <i>wR</i> <sub>2</sub> )	0.038, 0.100	0.055, 0.138	0.055, 0.158	0.454, 0.102	0.041, 0.096	0.042, 0.108
final <i>R</i> indices (all data) ( <i>R</i> <sub>1</sub> , <i>wR</i> <sub>2</sub> )	0.072, 0.244	0.111, 0.637	0.092, 0.203	0.143, 0.148	0.098, 0.137	0.094, 0.320
largest peak and hole (eÅ <sup>-3</sup> )	+0.16, −0.13	+0.27, −0.52	+0.38, −0.35	+0.26, −0.16	+0.25, −0.22	+0.28, −0.30

ArH), 7.23–7.30 (2H, m, ArH); <sup>13</sup>C NMR (CD<sub>3</sub>CN) δ 55.43, 61.27 (br), 68.63 (d, *J*<sub>CF</sub> = 1.4 Hz), 124.17 (d, *J*<sub>CF</sub> = 4 Hz, Ar), 130.39 (d, *J*<sub>CF</sub> = 13 Hz, Ar), 130.41 (d, *J*<sub>CF</sub> = 5.5 Hz, Ar), 161.90 (d, *J*<sub>CF</sub> = 250 Hz, Ar). **FN<sub>2</sub>O<sub>4</sub>·Ca(ClO<sub>4</sub>)<sub>2</sub>**: <sup>1</sup>H NMR (CD<sub>3</sub>CN) δ 2.76 (br), 3.23 (br), 3.81 (br), 4.23 (br), 7.30–7.38 (1H, m), 7.45–7.52 (2H, m); <sup>13</sup>C NMR (CD<sub>3</sub>CN) δ 54.39, 54.7–56.5 (br), 69.00, 70.53, 127.79 (d, *J*<sub>CF</sub> = 3.3 Hz), 128.26 (d, *J*<sub>CF</sub> = 12 Hz), 132.13 (d, *J*<sub>CF</sub> = 5 Hz), 158.87 (d, *J*<sub>CF</sub> = 230 Hz). **(FN<sub>2</sub>O<sub>4</sub>)<sub>2</sub>**: mp 129 °C; <sup>1</sup>H NMR (CDCl<sub>3</sub>) δ 2.77 (16H, t, *J* = 11.0 Hz, NCH<sub>2</sub>), 3.61–3.66 (32H, m, OCH<sub>2</sub>), 3.75 (8H, s, ArCH<sub>2</sub>), 6.83–6.91 (2H, m, ArH), 7.34–7.41 (4H, m, ArH); <sup>13</sup>C NMR (CDCl<sub>3</sub>) δ 52.40, 54.53, 69.88 (CO), 70.88 (CO), 123.58 (d, *J*<sub>CF</sub> = 4 Hz, Ar), 125.72 (d, *J*<sub>CF</sub> = 15 Hz, Ar), 129.69 (d, *J*<sub>CF</sub> = 5 Hz, Ar), 159.53 (d, *J*<sub>CF</sub> = 245 Hz, Ar); MS *m/z* 765.6.

**2-Fluoro-1,3-bis[(1-aza-4,7,10-trioxacyclododecyl)methyl]benzene (F(NO<sub>3</sub>)<sub>2</sub>), 2-Fluoro-1,3-bis[(1-aza-4,7,10,13-tetraoxacyclopentadecyl)methyl]benzene (F(NO<sub>4</sub>)<sub>2</sub>), and 2-Fluoro-1,3-bis[(1-aza-4,7,10,13,16-pentaoxacyclooctadecyl)methyl]benzene (F(NO<sub>5</sub>)<sub>2</sub>)**. A mixture of the respective aza crown ether (2 equiv), 1,3-bis(bromomethyl)-2-fluorobenzene (1 equiv), and Na<sub>2</sub>CO<sub>3</sub> (10 equiv) was heated under reflux for 24 h. The cooled reaction mixture was filtered and evaporated to dryness and the oily residue purified by chromatography (cyclohexane:ethyl acetate:diethylamine = 5:5:1). **F(NO<sub>3</sub>)<sub>2</sub>**: yield: 0.66 g (79%). <sup>1</sup>H NMR (CDCl<sub>3</sub>) δ 2.67 (8H, t, *J* = 4.8 Hz, NCH<sub>2</sub>), 3.53–3.62 (24H, m, OCH<sub>2</sub>), 3.66 (4H, s, ArCH<sub>2</sub>), 7.08 (1H, “t”, ArH), 7.40 (2H, “t”, ArH); <sup>13</sup>C NMR (CDCl<sub>3</sub>) δ 53.11, 54.58, 70.01, 70.49, 71.20, 123.33 (d, *J*<sub>CF</sub> = 4 Hz), 125.45 (d, *J*<sub>CF</sub> = 16 Hz), 130.05 (d, *J*<sub>CF</sub> = 5 Hz), 159.78 (d, *J*<sub>CF</sub> = 247 Hz). **F(NO<sub>4</sub>)<sub>2</sub>**: yield 0.59 g (60%); <sup>1</sup>H NMR (CDCl<sub>3</sub>) δ 2.77 (8H, t, *J* = 5.9 Hz, NCH<sub>2</sub>), 3.59–3.68 (32H, m, OCH<sub>2</sub>), 3.70 (4H, s, ArCH<sub>2</sub>), 7.00 (1H, “t”, ArH), 7.28 (2H, “t”, ArH); <sup>13</sup>C NMR (CDCl<sub>3</sub>) δ 53.00, 54.14, 69.82, 70.14, 70.46, 70.92, 123.25 (d, *J*<sub>CF</sub> = 4.5 Hz), 125.77 (d, *J*<sub>CF</sub> = 16 Hz), 129.74 (d, *J*<sub>CF</sub> = 5 Hz), 159.63 (d, *J*<sub>CF</sub> = 244.5 Hz). **F(NO<sub>5</sub>)<sub>2</sub>**: yield 0.17 g (88%); <sup>1</sup>H NMR (CDCl<sub>3</sub>) 2.75 (8H, t, *J* = 5.7 Hz, NCH<sub>2</sub>), 3.56–3.64 (40H, m, OCH<sub>2</sub>), 3.69 (4H, s, ArCH<sub>2</sub>), 6.99 (1H, “t”, ArH), 7.28 (2H, “t”, ArH).

**N-(3-Methylbenzyl)-1-aza-4,7,10,13-tetraoxacyclopentadecane (HNO<sub>4</sub>)**. A mixture of 1-(bromomethyl)-2-fluoro-3-methylbenzene (460 mg, 2.50 mmol), aza-15-crown-5 (550 mg, 2.50 mmol), and

Na<sub>2</sub>CO<sub>3</sub> (1.0 g) in acetonitrile (50 mL) was refluxed for 16 h. The mixture was filtered and washed with acetonitrile (25 mL) and the solvent evaporated *in vacuo*. The residue was subjected to silica gel column chromatography with cyclohexane–diethylamine (5:1) to give **HNO<sub>4</sub>** as a pale yellow oil (355 mg, 1.1 mmol, 44%, *R*<sub>f</sub> = 0.47). **HNO<sub>4</sub>**: <sup>1</sup>H NMR (CDCl<sub>3</sub>) δ 2.33 (3H, s, ArCH<sub>3</sub>), 2.79 (4H, t, *J* = 6.0 Hz, NCH<sub>2</sub>), 3.61–3.71 (18H, m, OCH<sub>2</sub>, ArCH<sub>2</sub>), 7.01–7.17 (4H, m, ArH); <sup>13</sup>C NMR (CDCl<sub>3</sub>) δ 21.35 (ArCH<sub>3</sub>), 54.18 (NC), 60.72 (ArC), 69.97 (CO), 70.17 (CO), 70.52 (CO), 70.98 (CO), 125.91 (Ar), 127.54 (Ar), 127.97 (Ar), 129.55 (Ar), 137.63 (Ar), 139.49 (Ar).

**N-(2-Fluoro-3-methylbenzyl)-1-aza-4,7,10,13-tetraoxacyclopentadecane (FNO<sub>4</sub>)**. A mixture of 1-(bromomethyl)-3-methyl-2-fluorobenzene (520 mg, 2.55 mmol), aza-15-crown-5 (560 mg, 2.55 mmol), and Na<sub>2</sub>CO<sub>3</sub> (1.0 g) in acetonitrile (50 mL) was refluxed for 16 h. The mixture was filtered and washed with acetonitrile (25 mL) and the solvent evaporated *in vacuo*. The residue was subjected to silica gel column chromatography with cyclohexane–diethylamine (5:1) to give **FNO<sub>4</sub>** as a pale yellow oil (690 mg, 2.02 mmol, 79%, *R*<sub>f</sub> = 0.40). Single crystals of **FNO<sub>4</sub>·NaClO<sub>4</sub>** were obtained by diffusion of diethyl ether into a solution of **FNO<sub>4</sub>** and NaClO<sub>4</sub> in acetonitrile. **FNO<sub>4</sub>**: <sup>1</sup>H NMR (CDCl<sub>3</sub>) δ 2.25 (3H, d, *J*<sub>CF</sub> = 2.1 Hz, ArCH<sub>3</sub>), 2.81 (4H, t, *J* = 6.0 Hz, NCH<sub>2</sub>), 3.61–3.71 (16H, m, OCH<sub>2</sub>), 3.73 (2H, s, ArCH<sub>2</sub>), 6.92–7.08 (2H, m, ArH), 7.20–7.27 (1H, m, ArH); <sup>13</sup>C NMR (CDCl<sub>3</sub>) δ 14.49 (d, *J*<sub>CF</sub> = 4.8 Hz, ArCH<sub>3</sub>), 53.13 (d, *J*<sub>CF</sub> = 2.5 Hz, ArCH<sub>3</sub>), 54.28 (CN), 69.95 (CO), 70.27 (CO), 70.59 (CO), 77.64 (CO), 123.24 (d, *J*<sub>CF</sub> = 4 Hz, Ar), 124.48 (d, *J*<sub>CF</sub> = 18.5 Hz, Ar), 125.74 (d, *J*<sub>CF</sub> = 15 Hz, Ar), 128.72 (d, *J*<sub>CF</sub> = 5 Hz, Ar), 129.95 (d, *J*<sub>CF</sub> = 5 Hz, Ar), 159.89 (d, *J*<sub>CF</sub> = 249 Hz, Ar); <sup>19</sup>F NMR (CD<sub>3</sub>CN) δ −123.30 (t, *J* = 7.1 Hz). **FNO<sub>4</sub>·NaClO<sub>4</sub>**: mp 153 °C; <sup>1</sup>H NMR (CD<sub>3</sub>CN) δ 2.27 (3H, d, *J* = 2.2 Hz, ArCH<sub>3</sub>), 2.61 (4H, t, *J* = 4.5 Hz, NCH<sub>2</sub>), 3.56–3.66 (16H, m, OCH<sub>2</sub>), 3.75 (2H, d, *J* = 1.0 Hz, ArCH<sub>2</sub>), 7.02–7.27 (3H, m, ArH); <sup>13</sup>C NMR (CD<sub>3</sub>CN) δ 13.21 (CH<sub>3</sub>), 52.19 (d, *J*<sub>CF</sub> = 1.5 Hz, ArCH<sub>2</sub>), 53.71 (NC), 67.50 (CO), 68.90 (CO), 69.37 (CO), 69.62 (CO), 123.67 (d, *J*<sub>CF</sub> = 16 Hz, Ar), 124.88 (d, *J*<sub>CF</sub> = 4 Hz, Ar), 126.19 (d, *J*<sub>CF</sub> = 18.5 Hz, Ar), 131.40 (d, *J*<sub>CF</sub> = 5 Hz, Ar), 132.35 (d, *J*<sub>CF</sub> = 5 Hz, Ar), 161.19 (d, *J*<sub>CF</sub> = 241 Hz, Ar); <sup>19</sup>F NMR (CD<sub>3</sub>CN) δ −123.30; <sup>23</sup>Na NMR (CD<sub>3</sub>CN) δ −2.6 (s, *ν*<sub>1/2</sub> = 84 Hz).

**21-Fluoro-3,6,9,12,15-pentaoxabicyclo[15.3.1<sup>1,17</sup>]heneicos-1(21),17,19-triene (FO<sub>5</sub>):** KORBu (920 mg, 8.2 mmol) and tetraethylene glycol (688 mg, 3.6 mmol) were dissolved in toluene (100 mL), and the resulting solution was heated under reflux for 1 h. A solution of 1,3-bis(bromomethyl)-2-fluorobenzene (1000 mg, 3.6 mmol) in toluene (40 mL) was then slowly added at room temperature while vigorously stirring. Stirring was continued for 12 h, after which the solution was heated under reflux for 2.5 h. The reaction mixture was allowed to cool to room temperature, the precipitate filtered off, and the solvent removed from the filtrate *in vacuo*. Distillation of the residue at 0.1 Torr and 200 °C afforded FO<sub>5</sub> (656 mg, 58%) as a colorless oil. FO<sub>5</sub>: <sup>1</sup>H NMR (CD<sub>3</sub>CN)  $\delta$  3.46 (8H, s, OCH<sub>2</sub>), 3.50–3.59 (8H, m, OCH<sub>2</sub>), 4.51 (4H, d,  $J = 1.1$  Hz, ArCH<sub>2</sub>), 7.07–7.15 (1H, m, ArH), 7.29–7.36 (2H, m, ArH), 68.05 (d,  $J_{CF} = 3.1$  Hz, ArCH<sub>2</sub>), 70.49 (CO), 71.09 (CO), 71.19 (CO), 124.47 (d,  $J_{CF} = 3$  Hz, Ar), 126.70 (d,  $J_{CF} = 16$  Hz, Ar), 132.38 (d,  $J_{CF} = 5$  Hz, Ar), 161.64 (d,  $J_{CF} = 250.5$  Hz, Ar); <sup>19</sup>F NMR (CD<sub>3</sub>CN)  $\delta$  -121.27 (t,  $J = 7$  Hz). FO<sub>5</sub>·LiClO<sub>4</sub>: <sup>1</sup>H NMR (CD<sub>3</sub>CN)  $\delta$  3.53–3.66 (16H, m, OCH<sub>2</sub>), 4.56 (4H, d,  $J = 1.0$  Hz, ArCH<sub>2</sub>), 7.10–7.18 (1H, m, ArH), 7.32–7.39 (2H, m, ArH); <sup>13</sup>C NMR (CD<sub>3</sub>CN)  $\delta$  68.54 (d,  $J_{CF} = 3.0$  Hz, ArCH<sub>2</sub>), 70.02 (CO), 70.40 (CO), 70.54 (CO), 70.77 (CO), 124.83 (d,  $J_{CF} = 4$  Hz, Ar), 126.25 (d,  $J_{CF} = 15$  Hz, Ar), 132.97 (d,  $J_{CF} = 5$  Hz, Ar), 161.82 (d,  $J_{CF} = 250.5$  Hz, Ar). FO<sub>5</sub>·NaClO<sub>4</sub>: mp 155 °C; <sup>1</sup>H NMR (CD<sub>3</sub>CN)  $\delta$  3.51–3.69 (16H, m, OCH<sub>2</sub>), 4.54 (4H, s, ArCH<sub>2</sub>), 7.11–7.19 (1H, m, ArH), 7.31–7.39 (2H, m, ArH), <sup>13</sup>C NMR (CD<sub>3</sub>CN) 69.38 (d,  $J_{CF} = 2.8$  Hz, ArCH<sub>2</sub>), 70.29 (CO), 70.58 (CO), 70.74 (CO), 71.23 (CO), 125.41 (d,  $J_{CF} = 4$  Hz, Ar), 126.73 (d,  $J_{CF} = 15.5$  Hz, Ar), 132.09 (d,  $J_{CF} = 5.5$  Hz, Ar), 161.98 (d,  $J_{CF} = 245$  Hz, Ar); <sup>23</sup>Na NMR (CD<sub>3</sub>CN)  $\delta$  -10.1 (s,  $\nu_{1/2} = 36$  Hz). FO<sub>5</sub>·KClO<sub>4</sub>: <sup>1</sup>H NMR (CD<sub>3</sub>CN)  $\delta$  3.55–3.60 (12H, m, OCH<sub>2</sub>), 3.66–3.71 (4H, m, OCH<sub>2</sub>), 4.54 (4H, s, ArCH<sub>2</sub>), 7.16–7.23 (1H, m, ArH), 7.36–7.43 (2H, m, ArH); <sup>13</sup>C NMR (CD<sub>3</sub>CN) 69.00 (d,  $J_{CF} = 2.7$  Hz, ArCH<sub>2</sub>), 70.67 (CO), 70.74 (CO), 70.83 (CO), 125.88 (d,  $J_{CF} = 4$  Hz, Ar), 126.92 (d,  $J_{CF} = 15.5$  Hz, Ar), 132.82 (d,  $J_{CF} = 5$  Hz, Ar), 160.99 (d,  $J_{CF} = 238$  Hz, Ar). FO<sub>5</sub>·RbSO<sub>3</sub>CF<sub>3</sub>: <sup>1</sup>H NMR (CD<sub>3</sub>CN)  $\delta$  3.55–3.61 (12H, m, OCH<sub>2</sub>), 3.67–3.71 (4H, m, OCH<sub>2</sub>), 4.52 (4H, s, ArCH<sub>2</sub>), 7.15–7.23 (1H, m, ArH), 7.36–7.43 (2H, m, ArH); <sup>13</sup>C NMR (CD<sub>3</sub>CN)  $\delta$  68.92 (d,  $J_{CF} = 2.5$  Hz, ArCH<sub>2</sub>), 70.43 (CO), 70.54 (CO), 70.64 (CO), 70.98 (CO), 125.77 (d,  $J_{CF} = 4$  Hz), 126.70 (d,  $J_{CF} = 15$  Hz), 132.90 (d,  $J_{CF} = 5$  Hz), 161.14 (d,  $J_{CF} = 248$  Hz). FO<sub>5</sub>·Ca(ClO<sub>4</sub>)<sub>2</sub>: <sup>1</sup>H NMR (CD<sub>3</sub>CN)  $\delta$  3.76–3.84 (16H, m, OCH<sub>2</sub>), 4.66 (4H, s, ArCH<sub>2</sub>), 7.18–7.25 (1H, m, ArH), 7.37–7.45 (2H, m, ArH); <sup>13</sup>C NMR (CD<sub>3</sub>CN)  $\delta$  69.68 (br), 70.69 (CO), 71.50 (CO), 125.94 (d,  $J_{CF} = 14.5$  Hz, Ar), 126.18 (d,  $J_{CF} = 3.5$  Hz, Ar), 132.66 (d,  $J_{CF} = 5.5$  Hz, Ar), 161.76 (d,  $J_{CF} = 241$  Hz, Ar). FO<sub>5</sub>·Sr(ClO<sub>4</sub>)<sub>2</sub>: <sup>1</sup>H NMR (CD<sub>3</sub>CN)  $\delta$  3.64–3.76 (12H, m, OCH<sub>2</sub>), 3.82–3.89 (4H, m, OCH<sub>2</sub>), 4.69 (4H, s, ArCH<sub>2</sub>), 7.26–7.33 (1H, m, ArH), 7.42–7.50 (2H,

m, ArH); <sup>13</sup>C NMR (CD<sub>3</sub>CN)  $\delta$  70.54 (d,  $J_{CF} = 2.5$  Hz, ArCH<sub>2</sub>), 70.61 (CO), 70.91 (CO), 71.33 (CO), 71.66 (CO), 126.87 (d,  $J_{CF} = 15$  Hz, Ar), 127.36 (d,  $J_{CF} = 3.3$  Hz, Ar), 132.55 (d,  $J_{CF} = 5$  Hz, Ar), 160.17 (d,  $J_{CF} = 236$  Hz, Ar). FO<sub>5</sub>·Ba(ClO<sub>4</sub>)<sub>2</sub>: <sup>1</sup>H NMR (CD<sub>3</sub>CN)  $\delta$  3.71–3.74 (14H, m, OCH<sub>2</sub>), 3.82–3.88 (4H, m, OCH<sub>2</sub>), 4.68 (4H, s, ArCH<sub>2</sub>), 7.28–7.35 (1H, m, ArH), 7.46–7.53 (2H, m, ArH); <sup>13</sup>C NMR (CD<sub>3</sub>CN)  $\delta$  70.03 (d,  $J_{CF} = 2.8$  Hz, ArCH<sub>2</sub>), 70.83 (CO), 70.98 (CO), 71.07 (CO), 71.19 (CO), 126.68 (d,  $J_{CF} = 15.5$  Hz, Ar), 127.48 (d,  $J_{CF} = 4$  Hz, Ar), 133.61 (d,  $J_{CF} = 5$  Hz, Ar), 159.59 (d,  $J_{CF} = 240$  Hz, Ar).

**5.2. X-Ray Crystal Structure Determinations (Table 5).** Suitable crystals were mounted on top of a glass fiber. X-ray data were collected on an Enraf-Nonius CAD4 diffractometer using Mo K $\alpha$  radiation (71.069 pm) and a graphite monochromator. All structures were solved (SHELXS-86)<sup>61</sup> and refined (SHELXL-93)<sup>62</sup> against  $I^2$ . In the structures described all non-hydrogen atoms (with the exception of a few oxygen atoms in disordered perchlorate groups) were refined using anisotropic temperature coefficients. The hydrogen atoms were refined with fixed isotropic temperature coefficients (riding model). An empirical absorption correction ( $\psi$  scans) was applied in all cases.

**Acknowledgment.** This work was supported by the Fonds der Chemischen Industrie, the Deutsche Forschungsgemeinschaft, and the Freiburger Wissenschaftliche Gesellschaft. We wish to thank cand.-chem. J. Weisner for preparative work, Dr. W. Deck and Dipl.-Chem. M. Ruf for collecting the X-ray data, Dipl.-Chem. A. Meissner for help with some NMR experiments, Dr. S. Steuernagel from the Bruker AG Karlsruhe for the <sup>19</sup>F MAS NMR, V. Brecht for several 2D NMR spectra, and Prof. Dr. H. Vahrenkamp for his support.

**Supporting Information Available:** Tables giving crystal data, structure refinement data, atomic coordinates, isotropic and anisotropic displacement parameters, and bond lengths and angles of all structures reported in this paper (29 pages). This material is contained in many libraries on microfiche, immediately follows this article in the microfilm version of the journal, can be ordered from the ACS, and can be downloaded from the Internet; see any current masthead page for ordering information and Internet access instructions.

JA952928A

(61) Sheldrick, G. M. *SHELXS-86, A Program for the Solution of X-Ray Crystal Structures*; Universität Göttingen: Göttingen, 1986.

(62) Sheldrick, G. M. *SHELXL-93, A Program for the Refinement of X-Ray Crystal Structures*; Universität Göttingen: Göttingen, 1993.